Graphical Abstract

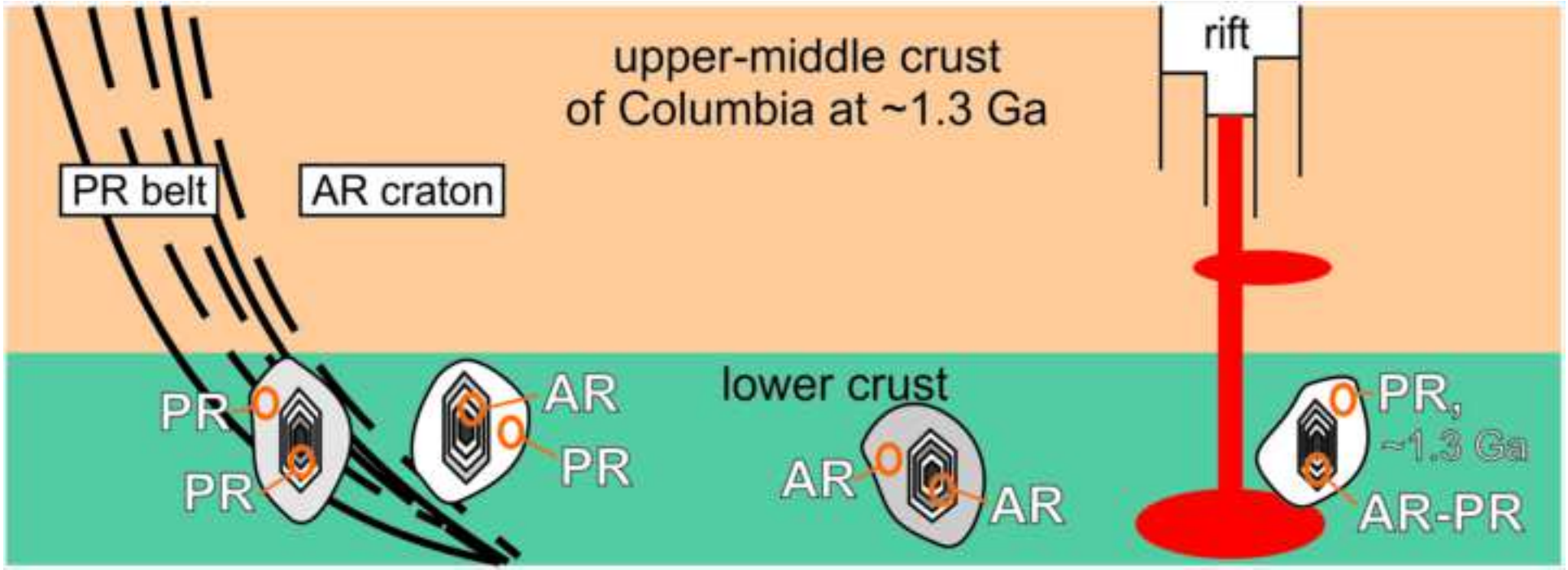

The highlights

- Proterozoic, mainly 1.9-1.7 Ga, granulitic lower crust predominates.
- A few regions preserved the Archean granulitic lower crust.
- U-Pb ages of metamorphic zircons reflect the slow cooling in the lower crust.

Gondwana Research Focus Review

The age of the lower crust of the Columbia supercontinent: a review of zircon data

Marina Koreshkova[1]*, Hilary Downes[2]

[1]*Institute of Earth Sciences, St Petersburg State University, Universitetskaya nab. 7-9, St Petersburg 199034, Russia, m.koreshkova@spbu.ru*

[2]*Department of Earth and Planetary Sciences, Birkbeck University of London, Malet Street, London WC1E 7HX, UK*

*Corresponding author: m.koreshkova@spbu.ru (M.Yu. Koreshkova)

Abstract

We have compiled data on textures, trace element contents, Hf isotope compositions and U-Pb ages of zircons from lower crustal xenoliths from the central part of the Columbia supercontinent in Precambrian areas in North America, Siberia and Northern Europe to address the question of when the host rocks to the zircons became part of the lower continental crust. The time when the lower crust reached its current state, a layer of high-pressure granulite-facies rocks, is dated by zircons that have equilibrated with garnet in

the observed metamorphic association. Zircons that have magmatic textures can provide the age of protolith crystallization, which did not necessarily occur within the lower crust. Magmatic zircons from within Archean cratonic areas of Columbia (the Slave, Wyoming, Superior, Siberian and Karelian cratons and the Archean Belomorian mobile belt in NW Russia) yield predominantly Archean ages (3.5-2.6 Ga). Addition of Proterozoic material may have occurred at craton boundaries and in areas of crustal extension but is rarely recorded in dated magmatic zircons that mainly have ages of 2.50-2.47 and 1.64 Ga. The granulite-facies association formed in Archean times has been preserved in lower crustal rocks of the Slave and Superior cratons despite later re-heating events. In other Archean areas of Columbia, the lower crust was reworked during Paleoproterozoic orogenic events. Nevertheless, sporadic surviving metamorphic zircons show that Archean lower crustal remnants are occasionally preserved. Mesoproterozoic extensional events and related magmatism occurred across a wide area at the southern margins of the Superior and Wyoming cratons, in the Belomorian belt, Yavapai and Mazatzal provinces and the Cheyenne belt. These events caused significant reworking of the lower crust with migmatization and formation of the granulite-facies association. The main differences of upper and lower crustal metamorphic histories are slow cooling and long duration of thermal events in the lower crust.

Keywords**:** lower crust, zircon, metamorphic history, protolith age, xenoliths, Columbia supercontinent

Content

1. Introduction

2. Interpretation of zircon ages

2.1. Zircon texture, trace element composition and Hf isotopes

2.2. Evaluation of zircon age data

3. Zircon data compilation

3.1. North America

3.1.1. The Slave craton

3.1.2. The Superior craton

3.1.3. The Wyoming craton and the Great Falls Tectonic Zone

3.1.4. The Medicine Hat block

3.1.5. The Cheyenne belt

3.1.6. The Proterozoic orogenic Yavapai and Mazatzal provinces

3.2. Northern Europe

3.2.1. The Karelian craton

3.2.2. The Belomorian Mobile Belt

3.3. Siberia

3.3.1. The Markha terrane, the Alakit field

3.3.2. The Markha terrane, the Daldyn field

3.3.3. The Markha/Daldyn terrane, the Muna field

3.3.4. The Markha terrane, the Nakyn field

4. Discussion

4.1. Protolith ages

4.2. Metamorphic history

4.3. Thermal history of the lower crust

4.4. The age of the lower crust of the Columbia supercontinent

5. Conclusion

1. Introduction

The nature and origin of the lower continental crust is a key problem in understanding Earth's crustal evolution (Rudnick and Gao, 2003). However, outcrops of the lower crust are difficult to access, other than in occasional upthrust regions such as the Ivrea zone in Italy and the Kohistan complex in Pakistan (Dhuime et al., 2007; Ewing et al., 2014, and references therein). The crust beneath Precambrian regions can be investigated via geophysical data and occasional xenoliths entrained in magmas that have passed through the lithosphere. In this study, we will use data from zircon-bearing lower crustal xenoliths to determine the timing of formation and metamorphic evolution of the lower crust beneath the present-day northern continents, which formed the central part of the Proterozoic supercontinent of Columbia (Evans and Mitchell, 2011; Meert, 2012; Meert and Santosh, 2017; Nance et al., 2014; Pesonen et al., 2012; Rogers and Santosh, 2002).

Data on mineralogy, chemical compositions and physical properties (density, seismic wave velocities etc.) obtained from xenoliths correspond to the state of the lower crust at the time of their entrainment in the host magmas. These data are usually consistent with geophysical information showing the state of deep crustal areas at the present day (e.g., Markwick et al., 2001; Kuusisto et al., 2006). However, the mineral assemblages of lower crustal rocks are much older, and most of them formed in the Proterozoic, with the notable exception of xenoliths from the North China craton (Liu et al., 2004; Su et al., 2017; Wei et al., 2015; Zheng et al., 2009)). In some areas, protoliths of lower crustal rocks can be as old as 3.5 Ga (Peltonen et al., 2006). Thus, mineral associations, major and trace element compositions

of minerals, mineral isochrons, U-Pb zircon dating and other data for xenoliths reveal different time slices of the geological history of the lower crust.

The lower continental crust may contain metaigneous rocks of different origins and ages, some of which probably formed at shallow depths (e.g., Koreshkova et al., 2011). Moreover, metasedimentary rocks are sometimes present among xenoliths (Zartman et al., 2012; Koreshkova et al., 2014, Aulbach et al., 2020). This points to tectonic burial of rocks that originated at or near the Earth's surface. Various processes have led to the present assemblage of lower crustal rocks, including tectonic transport, underplating of mantle magmas and intracrustal melting (Rudnick and Gao, 2003; Lee et al., 2006). Consequently, the protoliths' formation age may not coincide with the time of their emplacement within the lower crust.

Dating of the observed granulite-facies mineral associations determines the time of metamorphic transformation subsequent to the emplacement of protoliths, or the age of later superimposed events. The age of high-pressure granulite-facies reworking establishes the minimum time limit when various components had assembled at depths corresponding to the lower crust. In other words, it is the age of the lower crust as a distinct structural unit of the present-day continental lithosphere.

Rb-Sr and Sm-Nd mineral isochrons for lower crustal xenoliths (mostly Grt-granulites) do not give a real metamorphic age. Instead, they correspond to the time when ambient temperature was low enough to slow down isotope exchange (the "closure" temperature). Lu-Hf mineral isochrons can give a better estimate of metamorphic age due to the slow diffusion of Hf in garnet and clinopyroxene (e.g., Scherer et al., 2000). However, the difference in diffusivities of Hf and Lu and the zoning of minerals must be taken into account (Bloch et al., 2015). $^{207}Pb/^{204}Pb$ - $^{206}Pb/^{204}Pb$ mineral isochrons also show a wide range of age

estimates between the timing of metamorphism and the age of xenolith entrainment (e.g., Kempton et al., 2001). These estimates are often imprecise due to several phenomena that can easily disturb the Th-U-Pb isotope system (for example, the presence of zircon inclusions in garnet).

U-Pb dating of rutile can give the age of the onset of a steady-state cratonic geotherm within the lower crust due to its relatively low closure temperature (Cherniak and Watson, 2003; Schmitz and Bowring, 2003; Blackburn et al., 2011). In contrast, zircon can precisely date the formation of the observed granulite-facies mineral association if it equilibrated with minerals in this association. However, zircon sometimes preserves a record of earlier events, so its relationship to a given association should be carefully evaluated. Monazite is comparable to zircon in its resistance to high temperature (Cherniak and Watson, 2003). Titanite also has Pb diffusivities that are higher (Cherniak and Watson, 2003) or comparable to zircon (Kohn, 2017). The closure temperature for Pb in zircon exceeds 900^{o}C for a cooling rate ≥1^{o}C/Myr and a grain radius ≥50 μm (Dodson, 1973).

Whole-rock Sr-, Nd-, Hf- and Os model ages can serve to verify the protolith ages obtained from zircon. However, these isotopic systems can also be disturbed by metasomatism. Aulbach et al. (2010) demonstrated that Re-Os dating of primary sulfides from lower crustal granulites gives reliable protolith ages because sulfides are the major hosts of Os during their formation and remain so through metamorphic changes. Unfortunately, Re-Os isotope data for lower crustal rocks are scarce.

Lower crustal xenoliths from volcanics in Archaean cratons and Proterozoic orogenic belts in North America, Siberia and Northern Europe (Fig. 1) contain zircons with ages from 3.5 to 1.1 Ga (Table 1) that provide a record of magmatic and metamorphic events of this period. During the late Paleoproterozoic-Mesoproterozoic, these regions composed

the central part of the Columbia supercontinent (Meert, 2012; Meert and Santosh, 2017; Rogers and Santosh, 2002), also known as “Nuna” (Evans and Mitchell, 2011) or “Early Columbia” (Pesonen et al., 2012). The supercontinent was assembled from Archean and Paleoproterozoic blocks that collided around 1.9-1.7 Ga (Evans and Mitchell, 2011; Meert, 2012; Meert and Santosh, 2017; Pesonen et al., 2012; Rogers and Santosh, 2002), although Pesonen et al. (2012) suggested that accretion lasted much longer, from 1.9 to around 1.5 Ga. The breakup of the supercontinent occurred in the period between 1.5 and 1.3 Ga; however, numerous localized extensional events from as early as 1.8 Ga are recognized (Evans and Mitchell, 2011; Pesonen et al., 2012; Rogers and Santosh, 2002).

This study will review the ages of formation of the observed granulite-facies mineral association from data on metamorphic zircons and will examine earlier metamorphic events that may have occurred in the deep crust. For this purpose, we will consider mechanisms of subsolidus zircon formation since they affect the interpretation of dating results and we will evaluate mineral associations in equilibrium with zircon if sufficient data are available. We aim to evaluate the time when the zircon-bearing rocks formed the lower crust in its current state.

Our compilation includes data on texture, trace element (U, Th, Y, REE) contents, Hf isotope composition and U-Pb age of zircons from lower crustal xenoliths from Precambrian areas in North America, Siberia and Northern Europe (Fig. 1). The age data on metamorphic zircons belong mostly to the period of 1.9-1.3 Ga when these areas were different parts of the single Columbia supercontinent (Evans and Mitchell, 2011; Meert and Santosh, 2017; Nance et al., 2014; Pesonen et al., 2012; Rogers and Santosh, 2002).

Fig. 1. 1- or 1.5-column fitting image

2. Interpretation of zircon ages

We have included available information on zircon textures, ages and Hf isotopes in Table 1 and an extended table in ESM 1. In the referenced works, U-Pb dating of zircon was performed using different methods: (1) isotope dilution-thermal ionization mass spectrometry (ID-TIMS), including chemical abrasion of zircon grains before digestion (CA-ID-TIMS), (2) secondary ion mass spectrometry (SIMS), and (3) laser ablation-inductively coupled plasma mass spectrometry (LA-ICP-MS). Each technique has its advantages and restrictions (Schaltegger et al., 2015). In brief, TIMS gives the lowest analytical uncertainty but poor spatial resolution. SIMS and LA-ICP-MS are excellent at spatial resolution but measurement uncertainties are 1-3%. LA-ICP-MS is the fastest and most widely available method. However, the depth of a laser pit is about 10-20 μm, so an invisible volume is sampled which sometimes leads to the analysis of a mixture of different domains within a single zircon grain. We have included information on the applied methods in ESM 1.

We have also included data on ages of rutile and titanite (listed in ESM 1), since they reflect the thermal history of the lower crust, and bulk rock Hf and Nd depleted mantle model ages which are useful for evaluating the protolith ages. We did not include any data on zircon xenocrysts in magmatic rocks due to the large assumptions which must be made about their origin (e.g., Kostrovitsky et al., 2016). We also excluded data on outcropping rocks which were once equilibrated at lower crustal depths because formally they do not correspond to the present-day lower crust.

2.1. Zircon texture, trace element composition and Hf isotopes

Magmatic zircons usually form euhedral prismatic grains and show oscillatory- and sector-zoning or, less often, a homogeneous internal texture in BSE and CL (Corfu et al., 2003). Metamorphic zircon grains are mainly oval, rounded, or polygonal to irregular in shape, smooth or multifaceted. They have sector-zoned, planar, feathery or convoluted (with thin curved bands), and homogeneous internal textures in BSE and CL. Typical sector-zoning patterns are polygonal (sectors of polygonal shape) and “fir-tree” (sectors with zigzag boundaries and, sometimes, oscillatory zoning within sectors). The detailed description of these textures and examples can be found in Corfu et al. (2003). In some cases, magmatic and metamorphic zircons have a similar appearance. For example, magmatic zircons crystallized from small-volume residual melts can be anhedral; or large sectors in fragmented grains cannot definitely be ascribed to magmatic or metamorphic conditions. In addition, a primary magmatic texture can become blurred during later metamorphism. Obviously, additional information is needed to infer zircon origin. Data on mineral inclusions in zircon, trace elements and Hf isotopes can help in interpreting zircon origin and the results of dating (Rubatto, 2017).

The variety of compositions of magmatic zircons is related to the composition of parental magmas, the temperature of crystallization and oxygen fugacity (Burnham and Berry, 2012; Grimes et al., 2015, Claiborne et al., 2018; Loucks et al., 2018). Rubatto and Hermann (2007) argued that the influence of pressure is much smaller than that of temperature and melt composition. However, the role of pressure is to stabilize garnet that strongly affects the distribution of Y and HREE. In the same way, the composition of metamorphic zircons reflects the temperature of their formation and the composition of the material from which they crystallized. This material can be the rock as a whole, the

groundmass excluding some minerals (e.g., garnet), or a single mineral (e.g., pre-existing zircon or exsolution from rutile) (Ewing et al., 2014; Sláma et al., 2007). Experimental studies by Rubatto and Hermann (2007) and Taylor et al. (2014) provide an opportunity to evaluate equilibrium with garnet in the presence of partial melt. Generally, HREE and Y contents in co-existing garnet and zircon, and zircon/garnet distribution coefficients of these elements, decrease with increasing temperature. In the absence of melt, similar relationships are observed at lower temperatures (Rubatto, 2017). An example of internal texture and REE composition of different zircon generations from Grt-granulite xenolith from the Udachnaya kimberlite pipe, Siberia, is given in Fig. 2. In this sample, metamorphic zircon generations with homogeneous and convoluted textures could have equilibrated with garnet at 900-950^{o}C according to $D^{Zrn/Grt}$ from Rubatto and Hermann (2007).

Fig. 2. 1.5-column fitting image

Metamorphic zircon can be produced in net transfer reactions when the mineral association and/or mineral mode changes. In this case, zircon most probably forms during cooling when the solubility of Zr in garnet, clinopyroxene, amphibole and rutile decreases (Rubatto, 2017). These zircons often have sector-zoned or convoluted textures. Oxygen and Hf isotopes can provide information on the source material for zircon. The radiogenic Hf isotopic composition of subsolidus zircon may reflect a bulk rock isotopic composition that has evolved over time, or it may be less radiogenic if zircon formed from Lu-poor minerals, or highly radiogenic if previously formed garnet was involved in zircon formation. In our compilation, most of the sector-zoned (polygonal and “fir-tree”) and

convoluted zircons have Hf isotopic compositions that can be produced from evolved bulk rock compositions (Figs. 3 and 4).

Subsolidus zircon can also be formed by recrystallization as described by Schaltegger et al. (1999), Hoskin and Schaltegger (2003) and Hoskin and Black (2000). This zircon mostly forms replacement rims on older grains, or develops around defects and inclusions. It has a homogeneous texture, and sometimes preserves ghostly outlines of the older zircon texture. This type of zircon can partially retain older ages inherited from the previous generation (Hoskin and Black, 2000). Recrystallization proceeds by the diffusion of ions of minor constituents and the migration of point and linear defects through the zircon lattice (Poirier, 1985). It often leads to the removal of U, Th, Pb, REE and Y if the previous zircon was rich in these elements, and their concentrations are therefore out of equilibrium with the new conditions. Accordingly, the REE composition of recrystallized zircons reflects the conditions of its formation as in zircons produced in net transfer reactions. However, no growth of new zircon occurs (no external material was involved); so the εHf(t) of recrystallized zircon remains the same as that of its precursor. Most of the homogeneous zircons (possibly all CL-bright homogeneous zircons) in Figs. 3 and 4 were formed by recrystallization of previous generations of magmatic and metamorphic zircon.

Zircons with a (more or less) homogeneous texture can also be produced by dissolution-precipitation of an earlier zircon generation. This process is documented in metamorphic rocks that have experienced dehydration reactions (e.g., Gauthiez-Putallaz et al., 2016). In this case, zircon should have no ghost textures, but sometimes it can have a convoluted texture (samples Mk111, P5/354, Koreshkova et al., 2017).

2.2. Evaluation of zircon age data

Zircons belonging to the same generation, that is, having the same texture, trace element composition and Hf isotope composition, may show a wide spectrum of concordant or nearly concordant U-Pb ages. The younger ages can result from partial to complete resetting of the Th-U-Pb system, a problem that has long been discussed (e.g., Schaltegger et al., 1999, Hoskin and Schaltegger 2003, Levskii et al., 2003, and references therein). The problem concerns the rate of volume diffusion of Pb, which is about five orders of magnitude faster than that of U and Th (Cherniak and Watson, 2003) but not always fast enough to cause the age loss. However, as Watson and Cherniak (2013) showed, significant Pb-loss occurs during heating in addition to the loss during cooling. We consider that a heating-cooling event at lower crustal metamorphic conditions (temperature about 800-1000^{o}C, low cooling rate) can explain partial to complete resetting of previously-formed zircons. Other mechanisms of Pb loss apart from volume chemical diffusion can play a significant role. These include diffusion along dislocations, diffusion in migrating grain boundaries (Poirier, 1985) and enhanced diffusion during dislocation creep (e.g., Reddy et al., 2006; Kovaleva et al., 2014). Figs. 3 and 4 demonstrate a significant amount of reset magmatic zircons having various ages but a narrow range of initial Hf isotopic compositions.

Our analysis is based on zircon texture and composition, including Hf isotopes, i.e., on the mode of zircon formation. To define an equilibrium assemblage of minerals co-existing with a given zircon generation, we have used data on the types of mineral inclusions present in zircon and the HREE composition of the zircon. We paid special attention to identify mixed analyses of different generations where possible. Because of probable partial resetting of older zircon generations, we preferred the oldest ages for them except for dating results for zircons formed by recrystallization. The latter are most reliable if they form clusters on the

Concordia diagram. Therefore, some discrepancies with the original data interpretation are possible.

3. Zircon data compilation

A summary of the data is presented in Table 1 and ESM 1. Sample localities are shown in Fig. 1. Brief information on host rocks and local geological settings is given in ESM 2. Figs. 3 and 4 demonstrate available data on Hf isotopic compositions of zircons and whole rock samples of lower crustal xenoliths from the Belomorian mobile belt, the Wyoming craton and the Great Falls Tectonic Zone, the Yavapai and Mazatzal provinces, and the Siberian craton.

Table 1

3.1. North America

In North America, lower crustal xenoliths are found in kimberlites, lamprophyres and other potassic volcanic rocks in the Slave and Superior cratons, the Great Falls Tectonic Zone, the Wyoming craton, the Medicine Hat block, and in the Cheyenne, Yavapai and Mazatzal Proterozoic mobile belts (Fig. 1).

3.1.1. The Slave craton

Davis et al. (2003) reported the results of zircon dating using ID-TIMS and SIMS (SHRIMP) for xenoliths from kimberlite pipes in the central and southern Slave craton (ESM 2). In metagranitoid xenoliths, they obtained ages of 3.20-2.62 Ga from oscillatory-zoned

zircon cores (some of which may be inherited) and 2.64-2.56 Ga from metamorphic overgrowths and recrystallized rims. Magmatic zircons from mafic Grt-granulite xenoliths yielded ages of 3.02-2.56 Ga (the latter possibly reset). According to Os isotope data in sulfides (Aulbach et al., 2010), protoliths of lower crustal xenoliths from the central Slave craton may be as old as 3.3 Ga. The age of metamorphic zircons (rims, overgrowths and new-formed grains with sector zoning or homogeneous texture) is 2.60–2.51 Ga (Table 1, ESM 1). Antonelli et al. (2019) reported a $^{207}Pb/^{206}Pb$ age of 2528 ±9 Ma for metamorphic zircons containing inclusions of garnet from a lower crustal metapelite xenolith. The $^{207}Pb/^{206}Pb$ age of titanite from metagranitoids and mafic Grt-granulites indicates that the mineral associations have been preserved since 2.55 Ga (Davis et al., 2003). Rutiles from metagranitoids show ages between 1.94 and 1.81 Ga, whereas those from mafic Grt-granulites are dated at 1.39-1.06 Ga (Davis et al., 2003; Förster et al., 2017).

3.1.2. The Superior craton

Moser and Heaman (1997) studied zircons from three Pl-rich Grt-granulites and one Grt-clinopyroxenite xenolith from a kimberlite pipe near Kirkland Lake, Ontario, using ID-TIMS (Table 1, ESM 1, ESM 2). Most zircons are discordant. The oldest age of 2788 ±57 Ma from the upper intersection with the Concordia belongs to the zircon cores in Grt-granulite sample Z, showing oscillatory and sector-zoned texture in CL. The lower intersection and the analysis of a single CL-bright homogeneous rim gave indistinguishable ages: 2416 ±30 Ma and 2422 ±3 Ma, respectively. The data for a Grt-clinopyroxenite xenolith suggest that the zircon cores are older than 2633 ±3 Ma and overgrowths are younger than 2531 ±7 Ma. These zircons contain inclusions of clinopyroxene. In one Grt-granulite xenolith (sample X), two

zircon cores showed polygonal and fir-tree sector-zoning in CL, typical of subsolidus zircons, with $^{207}Pb/^{206}Pb$ ages of 2561 ±4 Ma and 2563 ±4 Ma. In this case, the oldest value of 2629 ±8 Ma from an oval colorless grain may correspond to another unidentified zircon generation, or to the age of sector-zoned metamorphic zircons if those two grains studied in CL were reset. Round multifaceted grains and prismatic grains, both structureless in BSE, from another Grt-granulite xenolith (sample W) showed nearly concordant ages of 2.58 and 2.50 Ga, and the lower intersection with the Concordia was at about 1.44 Ga.

In a Grt-granulite xenolith from the southern margin of the Superior craton in Upper Michigan (Table 1, ESM 1, ESM 2), metamorphic zircon generations have ages of 1104 ±42 and 1387 ±32 Ma (Zartman et al., 2012). The older generation is represented by prismatic grains with oscillatory zoning and is assumed to be migmatitic. Its formation could be due to 1.3-1.5 Ga anorogenic granite magmatism. The younger CL-bright homogeneous rims of rounded grains can be related to metamorphism caused by the 1.1 Ga Mid-Continent Rift flood basalt eruptions (Zartman et al., 2012). The zircon cores have patchy textures. Their ages vary from 2.31 to 1.01 Ga due to partial to complete resetting. An oval grain with oscillatory zoning gave a $^{207}Pb/^{206}Pb$ age of 3506 ±9 Ma. From the whole-rock composition and the various textures of zircon cores, it follows that this xenolith had a sedimentary protolith (Zartman et al., 2012).

3.1.3. The Wyoming craton and the Great Falls Tectonic Zone

The xenoliths discussed here come mainly from potassic alkali volcanics of the Bearpaw Mountains located in the Great Falls Tectonic Zone (GFTZ). The zone is a 1.86–1.71 Ga collisional belt that sutured together the Wyoming craton and Medicine Hat block (Harms

et al., 2004). Gorman et al. (2002) detected a northward-dipping reflector tracing the zone to mantle depths that is interpreted as a relic subduction zone. Hence, the xenoliths could be derived from the crust of both the GFTZ and the underthrust Wyoming craton (Fig. 1, ESM 2).

Bolhar et al. (2007) reported age data for zircons from a silica-rich granulite xenolith (Table 1, ESM 1). They obtained Archean ages for zircon cores and Paleoproterozoic ages for rims, with the high-U rims being the youngest: 1.85-1.76 Ga. Scherer et al. (2000) reported values of 1707 ±15 and 1268 ±34 Ma (upper and lower intersections with the Concordia) for zircons from a Grt-clinopyroxenite xenolith. These zircons are anhedral, lack oscillatory zoning in CL, and have Th/U about 0.1 that suggests they are metamorphic. Sm-Nd and Lu-Hf isochrons show that the minerals and the whole rock were in equilibrium. The Hf isotopic composition of this xenolith is more radiogenic than that of the depleted mantle (e.g., Vervoort et al., 2000). Possibly, this pyroxenite formed as a residue after partial melting (Fig. 3).

Barnhart et al. (2012) studied monazites from xenoliths of mafic Grt-granulite, Grt-Opx granulite and two Grt-Bt-gneisses from the same locality. Monazites were formed or recrystallized during several periods of metamorphism: 2.2-2.0 Ga, 1.89-1.81 Ga, 1.80-1.78 Ga, 1.75-1.71 Ga, 1.69-1.66 Ga and about 1.3 Ga. In the middle-crustal gneisses and in Grt-Opx-granulite, monazites formed between 1.80-1.78 and 1.75-1.71 Ga predominate. The lower crustal Grt-granulite contains only monazite with the age of 1.3 Ga, which was formed later than the granulite-facies association.

Thakurdin et al. (2019) dated zircons from two mafic Grt-granulites, two Grt-free granulites and an upper-middle crustal amphibolite xenolith using SIMS (Table 1, ESM 1). In Grt-granulite LSC 33, zircon data define a Discordia that has the upper and lower intercepts at around 3.2 and 1.7 Ga. The Hf isotopic composition of zircon cores confirms their ancient

age (Fig. 3). The youngest ages are found in CL-bright, low-Th and U domains. Zircons from Grt-granulite LSC 105 have sector-zoned to patchy cores and CL-dark homogenous overgrowths but show a single cluster on the Concordia that gives an age of 1772 ±8 Ma. Therefore, this age corresponds to the formation of subsolidus zircon and resetting of the older generation. Zircons from Grt-free granulite xenoliths LSC 72 and LSC 89 have CL-dark cores with homogeneous and patchy texture and rarely with faint, disturbed sector-zoning. We consider the value of 2.53 Ga in LSC 89 to be a minimum age of crystallization of magmatic zircon taking into account the poorly preserved magmatic texture. Zircon cores from xenolith LSC 72 show $^{207}Pb/^{206}Pb$ ages of 1.80-1.78 Ga, apparently reset, but cannot be older than 2.25 Ga according to their Hf DM model age (Fig. 3). Metamorphic rims and reset cores form clusters on the Concordia at 1838 ±6, 1791 ±5, 1775 ±10 and 1730 ±15 Ma.

Farmer et al. (2005) studied Grt-free granulite xenoliths from the Leucite Hills in the south Wyoming craton (Fig. 1, ESM 2). They obtained concordant or nearly concordant ages of 2.70-2.56 Ga and 1.07 Ga from equant to slightly elongate multifaceted zircons with oscillatory-zoned cores and homogeneous rims and domains. Mirnejad and Bell (2008) reported the depleted mantle Nd model ages of 3.78-2.66 Ga for similar samples from the same host lamproite body (Table 1, ESM 1).

3.1.4. The Medicine Hat block.

The basement of the Medicine Hat block is a fragment of an Archean continent that was sutured with the Wyoming and Hearne cratons by the Proterozoic GFTZ in the south and the Late Archean Vulcan structure in the north (Gorman et al., 2002; Chen et al., 2017) (Fig. 1, ESM 2).

Zircons from two xenoliths of middle crustal Grt-gneisses from potassic volcanics of the Sweetgrass Hills have been dated using CA-ID-TIMS (Blackburn et al., 2011). In one of them, zircon has relic magmatic cores with ages around 2.7 Ga. The other contains metamorphic zircons with homogeneous textures and an age of 1.8 Ga. Rutiles from these samples have discordant ages with the upper intersection with the Concordia at about 1.8 and 1.5 Ga whereas rutile from a zircon-free mafic Grt-granulite xenolith is about 1.0 Ga old (Table 1, ESM 1).

3.1.5. The Cheyenne belt

The Cheyenne belt is a ~1.8 Ga-old collisional belt at the southern margin of the Wyoming craton, bordering the Yavapai province to the south (Mueller and Frost, 2006; Rumpfhube and Keller, 2009). It is composed of Early Proterozoic and, possibly, reworked Archean rocks. At 1.4 Ga, anorogenic granitoid magmatism occurred in the region (Mueller and Frost, 2006). In the Neoproterozoic and in the Devonian, several kimberlite diatremes emplaced in the State Line district (Farmer et al., 2005, and references therein) (Fig. 1, ESM 2).

Zircons from Grt-granulite xenoliths from the State Line kimberlites vary in shape and color and show several periods of formation: 3.2-2.6 Ga, 1.7-1.6 Ga, 1.4-1.3 Ga and 0.5-0.4 Ga (Farmer et al., 2005). Zircons with Archean ages from upper crustal amphibolites and one lower crustal Grt-granulite are interpreted to be inherited. The major population of 1.74-1.60 Ga old zircons is shown by zoned grains having magmatic and metamorphic cores and rims (Table 1, ESM 1). In sample NX4-LC1, zircons have cores with patchy and fir-tree sector-zoning and homogeneous rims. This demonstrates the presence of two metamorphic

generations apart from the modified magmatic cores. Two grains with sector-zoning gave $^{207}Pb/^{206}Pb$ ages of 1379 ±2 Ma and 1343 ±2 Ma. Possibly, the homogeneous rims can be younger, otherwise the cores were reset. The patchy (magmatic) cores seem to be no younger than 1.72 Ga. In sample SD2-LC44, a single grain with oscillatory-zoned core and CL-bright rim yielded a $^{207}Pb/^{206}Pb$ age of 1720 ±3 Ma. Assuming that the material preferentially analyzed by TIMS belongs to the core, this value can be the age of crystallization from a melt.

3.1.6. The Proterozoic orogenic Yavapai and Mazatzal provinces

Crowley et al. (2006) studied zircon in lower crustal xenoliths from lamprophyres of the Navajo volcanic field on the Colorado Plateau (Table 1, ESM 1, ESM 2). This area is located at the boundary of the Yavapai (1.8–1.7 Ga) and Mazatzal (1.7-1.6 Ga) orogenic belts. Crowley et al. (2006) used ID-TIMS for dating of air-abraded zircon grains and grain fragments. In mafic xenoliths, zircon grains are of two types: rounded with CL-dark cores and CL-bright homogeneous rims, and polygonal to irregular grains with feathery or fir-tree sector-zoning. CL-dark cores have blurred sector-zoning or patchy texture and showed ages of 1.44-1.43 Ga. Metamorphic zircon generations have ages of 1.41-1.38 Ga. In sample KRM02-06, metamorphic zircon has the most radiogenic Hf (higher than the whole rock); hence, it might have formed from Grt breakdown (Fig. 3). In samples KRM02-07 and KRM02-32, metamorphic zircons have significantly less radiogenic Hf than the magmatic cores. If these rims were formed by net transfer, introduction of non-radiogenic material must have occurred under subsolidus conditions. However, if they were formed by recrystallization or dissolution-reprecipitation, they had much older precursors (DM Hf model age = 1.83-1.81 Ga) than the analyzed cores (Fig. 3); thus, an older zircon generation was missed. We believe

this situation needs further study since it may indicate an age of the magmatic protoliths older than 1.44 Ga.

In felsic Grt-granulite xenoliths, magmatic zircons with clear oscillatory zoning gave ages of 1.73-1.60 Ga (Crowley et al., 2006). Metamorphic generations are indicated by CL-bright homogeneous grains and rims or grains with feathery and sector zoning which show ages between 1.41 and 1.38 Ga (Crowley et al., 2006). In sample KTT02-01, metamorphic zircons have higher Hf isotope ratios than the magmatic cores. They might have formed from dissolving garnet or from evolved matrix of the rock, which is probably a restite from partial melting (Fig. 3).

Fig. 3. 1.5-2-column fitting image

3.2. Northern Europe

Lower crustal xenoliths in northern Europe are found in kimberlites in Finland (Karelia) and NW Russia (Arkhangelsk), and in ultramafic lamprophyres of the Belomorian mobile belt (Fig. 1, ESM 2).

3.2.1. The Karelian craton

Peltonen et al. (2006) and Hölltä et al. (2000) analyzed zircons in six mafic Grt-granulite xenoliths from kimberlite pipes in eastern Finland using SIMS (Table 1, ESM 1). The diatremes are located at the Karelian craton margin, which was reworked during the 1.9-1.8 Ga Svecofennian orogeny (Nironen, 2017). Three xenoliths contain zircons with oscillatory-zoned cores that gave Archean ages, up to 3532 ±10 Ma. Sample Ju11 has zircons with

oscillatory- and sector-zoned cores with $^{207}Pb/^{206}Pb$ ages between 2500 and 1808 Ma, perhaps indicating addition of Proterozoic material to the Archean crust. Zircon grains from the other two samples are homogeneous and show ages of 1.98-1.72 Ga, dating the formation of subsolidus zircon during metamorphic events. Peltonen et al. (2006) noted that the ages of 1.8-1.7 Ga are younger than metamorphic events in the upper crust. They linked the granulite-facies conditions at that time to mafic underplating responsible for post-orogenic granites and lamprophyre intrusions in the region.

3.2.2. The Belomorian Mobile Belt

The Belomorian Mobile Belt is the late Archean suture between the Kola composite terrane and the Karelian craton, but it has strong imprint of the early Proterozoic Lapland-Kola orogeny (Balagansky et al., 2015; Bibikova et al., 2001, 2004; Daly et al., 2006; Glebovitskii et al., 2001, 2009; Mints et al., 2007, 2014; Nironen, 2017). Zircons from upper crustal xenoliths preserve Archean ages (Claesson et al., 2000). Zircons from lower crustal xenoliths were studied by Downes et al. (2002), Vetrin et al. (2009, 2018) and Koreshkova et al. (2014, 2017) using SIMS. In general, magmatic zircons with clear oscillatory zoning show ages from 2.84 to 2.72 Ga. The oldest value may belong to an inherited zircon grain because other zircons in this xenolith are about 2.47 Ga old (Downes et al., 2002). A magmatic zircon from a Phl-Prg-clinopyroxenite has an age of 1640 ±11 Ma, and represents a later small-volume addition to the lower crust (Koreshkova et al., 2017).

Metamorphic zircons preserved the record of events from ≥2.25 Ga to 1.27 Ga that can be divided into five periods: >1.91 Ga, 1.86–1.81 Ga, 1.77–1.74 Ga, 1.67–1.64 Ga, and <1.6 Ga (Koreshkova et al., 2017). Several xenoliths contain 2-4 generations of zircon. In

some of them, HREE compositions of the youngest zircon generations suggest that they were in equilibrium with existing garnets. Consequently, these zircons date the formation of the observed granulite-facies assemblages, which occurred 1.84-1.81 Ga ago (samples 60/473, P5/354, 77/690 and Mk260), 1.76 Ga ago (Mk111) and 1.64 Ga ago in Mk326 (Table 1, ESM 1). In Grt-granulite Mk326, pre-existing zircon has much lower HREE content (Yb_N/Dy_N = 0.6) than the latest one (Yb_N/Dy_N = 2.1) and was formed in the presence of garnet at high temperature and pressure. Hence, the event at 1.64 Ga was superimposed onto the granulite-facies association formed at 1.77 Ga or earlier. Similarly, in Grt-granulite xenolith Mk523, the 1.74 Ga old zircon dates the high-pressure metamorphic association which changed later, during metamorphic pulses over the period 1.6-1.3 Ga. The event at 1.67-1.64 Ga also largely affected Grt-pyroxenites and the eclogite Mk284.

The oldest age of 2.25 Ga is found in CL-dark sector-zoned metamorphic zircon in Grt-granulite xenolith Mk111. Other zircons of this generation were reset at 1.86-1.48 Ga. The age of 2.25 Ga might also be the result of partial resetting. This zircon has a very low Y and HREE content (Yb_N/Dy_N = 0.4), so it was equilibrated with abundant garnet at high pressure. Similar low-HREE zircon (with Yb_N/Dy_N as low as 0.2) was described in the Dora-Maira whiteschists in the Alps that experienced ultrahigh-pressure metamorphism (Gauthiez‐Putallaz et al., 2016). Hf isotopic composition of the zircon from sample Mk111 may correspond to a bulk rock composition evolved since about 3.3-2.8 Ga (Fig. 3). This points to a >2.25 Ga event within a thick crust that pre-dates the Lapland-Kola orogeny. Taking into account the possibility of formation under ultra-high pressure, it could have happened during the 2.9-2.6 Ga Belomorian orogeny.

3.3. Siberia

Numerous kimberlite diatremes sampled the lower crust of the Anabar and Olenek provinces of the Siberian craton (Rosen et al., 2006). Zircons from lower crustal xenoliths from the Olenek province have not been dated yet. The general distribution of crustal ages of this province is shown in the study of zircon xenocrysts from kimberlites (Kostrovitsky et al., 2016). The Anabar province consists of the Magan, Daldyn and Markha terranes (Rosen et al., 2006; Pisarevsky et al., 2008). The data on zircon age, texture and composition are available for xenoliths from the Alakit, Daldyn, Muna and Nakyn kimberlite fields within the Markha terrane (Fig. 1, ESM 2). The fields are listed with increasing distance from the Kotuykan suture zone between the Magan terrane and the Daldyn and Markha terranes. Possibly, the Muna field is located within the Daldyn terrane near the border with the Markha terrane (Rosen et al., 2006). The Markha terrane has thick Riphean-Cretaceous sedimentary cover containing Triassic basaltic traps. The geological history of the basement is not constrained in detail, so we have also taken into consideration the data reported for middle to upper crustal xenoliths.

3.3.1. The Markha terrane, the Alakit field

Shatsky et al. (2016) reported LA-ICP-MS data for zircons from one lower crustal mafic Grt-granulite and six middle crustal Grt-Bt- gneissose xenoliths from the Alakit field (Table 1, ESM 1). The Grt-granulite xenolith contains metamorphic low-Th and U zircons without clear zoning that show discordant ages with the average $^{207}Pb/^{206}Pb$ age of 1859 ±13 Ma. Zircons from two of the gneiss xenoliths have cores with blurred oscillatory zoning that differ in age and Hf isotopic composition; thus, they may be detrital zircons in

metasedimentary rocks, or inherited zircons in metagranitoids, or some of them can be migmatitic zircons in either rock type. These cores yield ages between 2.88 and 2.47 Ga. The younger values can be the result of resetting because zircons with different ages have the same Hf isotopic composition (ESM 1, ESM 3). Gneisses contain abundant subsolidus zircons as rims and overgrowths or individual grains with various zoning types. All samples demonstrate a spread of concordant ages between 1.98 and 1.80 Ga. From Th and U contents and Hf isotopic compositions, we suggest that there are two or more metamorphic zircon generations in each xenolith. For example, in K-69-02, there are at least two subsolidus zircons: an older, possibly 1.98 Ga old, with high Th/U (>1.1) and εHf(t)=0.1-0.8, and a younger one (1.88-1.89 Ga), high-U, with low Th/U (0.02-0.38) and εHf(t)=1.5-5.1 (ESM 3).

Here we present new age data for a mafic Grt-granulite xenolith Kom70 from Komsomolskaya kimberlite described by Koreshkova et al. (2011). This xenolith contains abundant baddeleyite (approximate age is 1.7 Ga) and only a few zircon grains. The latter are polygonal in shape, with a homogeneous to faint sector-zoning in CL, and with a low Th, U and HREE content. Their $^{207}Pb/^{206}Pb$ ages vary from 1643 to 2039 Ma. Three zircons form a cluster on the Concordia and give the age of 1656 ±27 Ma (Table 1, ESM 1, ESM 4). Their uniform texture and composition suggest that these grains belong to the same generation. We think that this zircon is metamorphic, formed ≥2.04 Ga ago, and reset at 1.66 Ga.

3.3.2. The Markha terrane, the Daldyn field

Koreshkova et al. (2009) studied zircons from eight lower crustal mafic Grt-granulite xenoliths and one middle crustal kinzigite xenolith from the Daldyn field, using SIMS (Table 1, ESM 1). Zircons from the Grt-granulites have magmatic cores 3.15-2.71 Ga old and

metamorphic rims formed between 1.94 and 1.81 Ga ago. CL-bright homogeneous zircons from samples Y7 (1.90 Ga old) and Y6 (>1.85 Ga old) were not in equilibrium with the observed garnets (garnet compositions are from Koreshkova et al. (2011)). The 1.87-1.84 Ga old convoluted overgrowths from samples Y6, Y7 and Uk37 could have equilibrated with garnet in the presence of a partial melt (Rubatto and Hermann, 2007). An example of calculations of zircon composition in equilibrium with garnet is shown in Fig. 2. Thus, the overgrowths date the granulite-facies association whereas the younger 1.83-1.81 Ga homogeneous zircons may reflect later recrystallization. The kinzigite xenolith contains abundant subsolidus zircons of two generations that yield the age of metamorphic events at 1936 ±6 and 1894 ±5 Ma.

Shatsky et al. (2016) analyzed zircons from three mafic Grt-granulite xenoliths from Daldyn kimberlites using LA-ICP-MS. In two of them, zircons have cores with ages of 2.53 and 1.98 Ga (Table 1, ESM 1). The older ages belong to the cores with a patchy texture that may be modified magmatic zoning. From Hf isotopic composition of zircon, the protolith of this sample (UD-01-44) could be as old as 3.0 Ga (Fig. 4). The younger age belongs to sample L-9-02, in which zircons are of two types: those with relatively radiogenic Hf, T_{DM} Hf = 2.3-2.4 Ga, and a single grain with T_{DM} Hf = 2.7 Ga. The latter is probably a relic magmatic core with a rejuvenated age. The BSE image shows a nearly homogeneous texture of the core with radiogenic Hf (Shatsky et al., 2016), thus it could be metamorphic in origin. A single analyzed rim gave an age of 1877 ±12 Ma. Therefore, this Grt-granulite xenolith records two metamorphic events at around 1.98 and 1.88 Ga. The third xenolith (UD-01-66) contains a single generation of metamorphic zircon with an age of 1792 ±14 Ma and εHf(t)=0.7-1.7. We believe that the latest metamorphic generations date the granulite-facies association; however, the radiogenic Hf isotopic composition in UD-01-66 and L-9-02 may point to a

retrograde path because of possible garnet breakdown that supplied radiogenic Hf (Fig. 4, ESM 3).

Fig. 4. 1.5-column fitting image

Moyen et al. (2017) reported age (LA-ICP-MS) and Hf isotope composition data for nine upper to middle crustal and six lower crustal xenoliths from Daldyn kimberlites (Table 1, ESM 1). The latter are mafic Grt-granulites; two of them are amphibole-rich. Three Grt-granulite xenoliths contain zircons with cores that retained ages of 2.88-2.66 Ga. In Grt-granulite 01-34, the cores have magmatic oscillatory texture. In amphibole-rich Grt-granulites, the texture is not specified. Metamorphic zircons from Grt-granulite xenoliths show ages of 1.85-1.83 Ga. In sample 02-34, zircons show polygonal to fir-tree sector-zoning in CL. Their Hf isotopic composition is more radiogenic than in zircons from Grt-granulites 02-36 and 01-106 described as being similar in texture (Fig. 4, ESM 3). Distinct mechanisms of formation and source materials can be suggested for these zircons: growth from the groundmass for samples 02-34 and 01-106, and recrystallization or dissolution-precipitation of a previous zircon generation for sample 02-36. The latter requires an Archean precursor. Xenoliths of upper crustal felsic Grt-free granulites, plagiogneisses and an amphibolite contain zircons with oscillatory cores and homogeneous rims. The cores have Archean ages (2.74-2.71 Ga) and the rims are Paleoproterozoic, around 1.87 Ga (ESM 1).

Shatsky et al. (2019) studied zircons from xenoliths of middle crustal Grt-free granulites and amphibolites and one lower crustal mafic Grt-granulite from the Daldyn field (Table 1, ESM 1). Zircons from the latter have magmatic cores that retained the age of 2.58 Ga but can be much older, given their blurred and disturbed texture and Hf isotopic composition (Fig. 4, ESM 3). Metamorphic rims of oval and rounded grains are homogeneous and bright in CL. Polygonal grains have overgrowths with CL-bright convoluted texture. The

two metamorphic generations were not analyzed separately; possibly, the youngest ages of 1.83-1.80 Ga correspond to the overgrowths. Some of the rims show a strong decrease in HREE concentrations, suggesting that they formed in the presence of garnet. Zircons from amphibolite xenoliths have oscillatory-zoned cores of 2.77 Ga and CL-bright convoluted to homogeneous rims. The variations in Hf isotopic composition and textural features suggest that there are two different generations in the cores that were partially reset at 1.86 Ga when metamorphic rims were formed. In Grt-free granulite xenoliths, zircons show partial resetting of magmatic ages and the formation of metamorphic rims at around 2.8-2.6 Ga and 1.9 Ga. This indicates a strong imprint of events at 1.9-1.8 Ga and the likelihood of preserving the Late Archean metamorphic history in middle crustal rocks.

3.3.3. The Markha/Daldyn terrane, the Muna field

Rosen et al. (2006) studied zircons from a two-pyroxene-Grt-granulite xenolith using TIMS (Table 1, ESM 1). Zircon fractions gave discordant ages with upper and lower intersections with Concordia at 3194 ±28 Ma and 1856 ±27 Ma, respectively.

Shatsky et al. (2018) analyzed zircons from two middle-lower crustal Grt-granulite xenoliths and one Grt-free granulite xenolith from Muna kimberlites, using LA-ICP-MS (Table 1, ESM 1). Zircons have magmatic oscillatory-zoned cores and homogeneous rims. Some grains are completely homogeneous in CL/BSE. The cores with concordant ages cluster at 2731 ±11, 2716 ±10 and 2714 ±7 Ma. The oldest concordant age value is 2740 Ma. εHf(t) values in the cores differ significantly (ESM 1, ESM 3). We suggest that there are either abundant inherited zircons with low εHf(t) or these rocks are metasedimentary in origin. Grains with homogeneous texture (Fig. 6 in Shatsky et al., 2018) retained Archean ages, the

significance of which is not clear. Unfortunately, the metamorphic history of these rocks was not studied.

3.3.4. The Markha terrane, the Nakyn field

Zircons from two middle-lower crustal Grt-granulite xenoliths were dated by Shatsky et al. (2018) using LA-ICP-MS (Table 1, ESM 1). In Grt-granulite Bt-39-03, the BSE-bright cores with the highest Th and U contents for this sample show $^{207}Pb/^{206}Pb$ ages from 2.77 to 2.27 Ga, apparently partially reset. Zircon cores from sample Bt-7-03 show concordant ages varying from 2.94 to 2.63 Ga. These cores differ in morphology: there are elongated subprismatic homogeneous grains, from which the oldest age of 2942 ±12 Ma was obtained, and oscillatory-zoned cores of oval and rounded grains. The latter have ages up to 2.89 Ga. Ten grains form a cluster on the Concordia at 2782 ±9 Ma. εHf at this age vary from -2.5 to 3.1, with the oldest subprismatic zircons in the middle of the data array (ESM 1, ESM 3). This xenolith deserves more careful study because more than two types of zircon cores may be present in it and the different metamorphic generations were not analyzed. Nevertheless, in xenolith Bt-39-03, homogeneous zircons with low Th and U (possibly the same as in rims) were analyzed. Presumably, these zircons are metamorphic grains without magmatic cores. They show ages from 2.0 to 2.7 Ga and have the same Hf isotopic composition as the magmatic cores. Unfortunately, the data are not sufficient to decide whether they are zircons recrystallized later than 2.0 Ga, or partially reset Archean metamorphic generations.

We have analyzed zircons from two lower crustal mafic Grt-granulite xenoliths and an upper crustal Hbl-Bt-Pl-gneiss xenolith from the Nakyn field (Table 1, ESM 1, ESM 4). A few zircons separated from the mafic Grt-granulites are small, polygonal in shape, and have

convoluted texture or fir-tree sector-zoning. REE composition is characterized by low HREE contents and Yb_N/Dy_N=0.9-3.2 (ESM 4) that suggests that these zircons grew together with garnet. Zircons yielded concordant ages of 1.85 and 1.88 Ga. Two spots gave a younger age of 1.83 Ga.

Little is known about metamorphism of upper crustal basement rocks in this area (Rosen et al., 2006). To have data for comparison, we dated the latest metamorphic generation of zircon from a plagiogneiss xenolith Nur26. This generation comprises CL-bright homogeneous grains and grain rims. Seven of the twelve spots form a cluster on the Concordia and yield the age of 2758 ±9 Ma (ESM 1, 4). Two analyzed magmatic cores of different types are 2.76 and 2.87 Ga old.

4. Discussion

4.1. Protolith ages

The data compilation demonstrates that magmatic zircons of the lower crust of the Archean nuclei of the Columbia supercontinent have predominantly Archean ages corresponding to the main stages of crustal growth (Table 1, Fig. 5, ESM 2). Initial Hf isotopic compositions of magmatic zircons is within the range of bulk rock compositions, supporting their crystallization from similar magmas (Figs. 3 and 4). Two xenoliths, one from Karelia (Peltonen et al., 2006) and one from the Belomorian belt (Downes et al., 2002), have ages around 2.5 Ga that may be related with a period of extension of the cratonic crust of the Baltic shield at this time (e.g., Nironen, 2015). One example of the addition of younger material to

the lower crust is a Phl-clinopyroxenite xenolith from the Belomorian belt (Koreshkova et al., 2017) which contains 1.64 Ga old magmatic zircons.

Fig. 5. 1.5-2-column fitting image

The lower crust of Proterozoic orogenic belts in North America can be investigated using xenoliths from the Bearpaw Mountains (Thakurdin et al., 2019a, b), the Navajo volcanic field (Crowley et al., 2006) and the State Line kimberlites (Farmer et al., 2005). The latter have 1.72 Ga old and older (≥1.74 Ga) magmatic protoliths and may represent juvenile rocks of the Cheyenne belt. In xenoliths from the Bearpaw Mountains, magmatic zircons show both Archean and Paleoproterozoic ages (Table 1, Fig. 5, ESM 1). Paleoproterozoic zircons were found in upper-middle crustal amphibolite and Grt-free granulite xenoliths. These xenoliths may originate from the juvenile crust of the GFTZ, while others with Archean protoliths may be reworked ancient rocks from the GFTZ or from the underlying Wyoming craton.

In felsic Grt-granulite xenoliths from the Navajo volcanics, magmatic zircons retained ages of 1.73-1.64 Ga. These dates are consistent with the age of juvenile upper crustal rocks of the Yavapai and Mazatzal provinces (ESM 2). Zircons from lower crustal xenoliths also show a strong influence of granitoid magmatism at 1.4 Ga: metamorphism with resetting of magmatic and metamorphic zircons and growth of new metamorphic zircon generations.

Crowley et al. (2006) suggested that the mafic Grt-granulite xenoliths in the Navajo volcanics were formed by magmatic underplating at ~1.4 Ga. In these xenoliths, U-Pb zircon age of 1.43 Ga is younger than the DM Hf model age, which was interpreted as the result of contamination of basaltic magmas with 1.7 Ga granitoids or felsic granulites. However, in three xenoliths, metamorphic zircons have much less radiogenic Hf than

magmatic cores, pointing to a non-radiogenic source material such as an older zircon generation (Fig. 3). This core-rim relationship is unusual and deserves further study. It requires either the introduction of non-radiogenic material under subsolidus conditions, or, more likely, an older zircon generation. Therefore, it cannot be ruled out that mafic Grt-granulite xenoliths may contain older magmatic zircons and be older than 1.43 Ga.

In some cases, xenoliths contain inherited zircons. This is significant because it indicates the presence of an older crust at the time of magmatic protolith emplacement. Such inheritance is evident for Grt-granulite 60/473 from Arkhangelsk (NW Russia) where zircons have oscillatory overgrowths on sector-zoned cores. It was also proposed for the oldest grain in Grt-granulite xenolith N39 from the Belomorian belt. It is also probable in xenolith L88 from Finland, in which two textural types are present in zircon grain cores. Inheritance can be revealed by the presence of magmatic grains with different Hf isotopic composition, for example, as observed in xenoliths from the Muna field in Siberia (Table 1, ESM1 and 3).

Nd and Hf DM model ages give some reassurance that the magmatic protoliths are as old as the zircons in them. We have included available data in Table 1. In many cases, zircon U-Pb ages and Nd-Hf DM model ages do not fundamentally contradict each other. The main reason for most discrepancies between them is not in the origin of protoliths or zircon inheritance but in contamination by the host magmas. For example, Koreshkova et al. (2011) showed that xenoliths from the Daldyn kimberlite field had experienced various degrees of contamination with host kimberlite and related fluids. In that study, one of the most altered and contaminated granulite xenoliths (sample Y7) had a Nd DM model age of 1.34 Ga, which is younger than the age of metamorphic zircons from the xenolith. Leaching experiments and calculated bulk rock compositions showed that contamination had also occurred in other, less altered xenoliths, and affected concentrations of LILE, LREE, Th and U.

Another problem when considering model ages is that lower crustal rocks could have experienced partial melting. A two-stage model would therefore be more appropriate if any constraints can be placed on time and degree of melting. However, in Grt-granulites of basic composition, a small-degree melting does not change Sm/Nd ratio significantly (Koreshkova et al., 2011).

Little can be said about the conditions of zircon crystallization from melts that formed the protoliths of lower crustal rocks. Some rare pieces of evidence are the basic Fe-rich xenoliths from Upper Michigan kimberlites (Zartman et al., 2012) and the Udachnaya pipe in Siberia (Koreshkova et al., 2011). The protolith melts of these rocks followed a tholeiitic path of crystal fractionation that constrains the depth of crystallization to be less than 0.7-0.8 GPa (Villiger et al., 2007). Pressure estimates for the granulite-facies associations from these localities are 0.9-1.2 GPa. This indicates tectonic transport of shallow rocks into the lower crust.

A few rare lower crustal rocks have metasedimentary protoliths. A metapelite xenolith from the central Slave craton was studied by Antonelli et al. (2019). A metasedimentary origin was inferred from bulk rock compositions and zircon data for a few mafic Grt-granulite xenoliths from elsewhere (samples P5/354 from Arkhangelsk (Koreshkova et al., 2014) and S69-5 from Michigan (Zartman et al., 2012)). In these xenoliths, the cores of zircons have different textures and trace element compositions, and these textural types are not observed within the same grain, but grains with different cores have identical metamorphic rims. The presence of metasedimentary rocks points unambiguously to tectonic burial as one of the mechanisms of formation of the present-day lower crust.

4.2. Metamorphic history

The oldest metamorphic events are recorded in mafic and felsic Grt-granulite xenoliths from the Slave craton, where the formation of metamorphic zircons occurred at 2.63-2.62 Ga and 2.58-2.51 Ga. In general, it was approximately contemporaneous with late- and post-accretion granitoid magmatism and crustal thickening (Davis et al., 2003; Helmstaedt, 2009) but some metamorphic zircons are noticeably younger, up to 2.51 Ga. The age of the youngest metamorphic generations of zircon is similar to that of titanite, indicating that the observed mineral association has been preserved since ~2.6 Ga (Davis et al., 2003).

Zircons studied by Davis et al. (2003) did not respond to later events (or there is a sampling bias) but the ages of titanite and rutile show that these minerals experienced Pb-loss or formed or recrystallized at ~1.7 Ga and 1.4-1.1 Ga. The youngest values may be associated with the 1.27 Ga Mackenzie dyke swarm event (Davis et al., 2003; Förster et al., 2017).

Grt-granulite xenoliths from the Abitibi subprovince, Superior craton, show Late Archaean-Early Proterozoic ages of metamorphic zircon overgrowths (2.58-2.42 Ga) (Moser and Heaman, 1997). These authors proposed that granulite-facies metamorphism occurred during extension and magma intrusion into the continental crust due to the opening of the Matachewan Ocean. One xenolith also contains metamorphic zircons dated at 1.44 Ga. This metamorphic event was related to the Grenville orogeny that affected the western margin of the Superior craton (Moser and Heaman, 1997), superimposed onto the granulite-facies association which had formed no later than 2.4 Ga ago.

Metamorphic zircons formed at 1.9-1.7 Ga are the most abundant in the lower crust of Columbia (Fig. 5), occurring in the Anabar province of the Siberian craton, the northern Wyoming craton, the Belomorian Mobile Belt and the Karelian craton (Table 1, ESM

1). Most researchers relate zircon-forming metamorphic events in the lower crust to collisional settings along the margins of Archaean terranes at that time (Bolhar et al., 2007; Koreshkova et al., 2009, 2014, 2017; Peltonen et al., 2006; Rosen et al., 2006; Shatsky et al., 2016; Thakurdin et al., 2019). The amalgamation of these terranes led to the formation of the Columbia supercontinent. Most of the xenolith localities are situated near Paleoproterozoic suture zones except for the Nakyn field in Siberia, which is in the center of the Markha terrane. The geology of its basement has not been studied in detail. However, the porphyroclastic texture of Grt-granulite xenoliths from this field (ESM 4) suggests the presence of a shear zone.

Peltonen et al. (2006) noted that, in Karelian xenoliths, zircon formation at 1.8-1.7 Ga post-dates Svecofennian orogenic events. Nironen (2017) showed that pegmatites and migmatite leucosomes with ages of 1.80–1.76 Ga are widespread in Fennoscandia, indicating that late metamorphism may have been associated with post-collisional crustal extension. The source of heat for this metamorphic event may have been intrusion of magmas at the base of the crust that led to the formation of post-collisional granitoids and lamprophyres.

In xenoliths from NW Russia, post-collisional ages range from 1.85 to 1.27 Ga, requiring multiple extensional events. The event at ~1.65 Ga is younger than intrusions of lamprophyres at the southwestern margin of the Karelian craton (1.79-1.78 Ga, Woodard et al., 2014, and references therein) and those within the Lapland Granulite Belt (1.72 Ga, Nikitina et al., 1999). It may be related to the onset of Mesoproterozoic rifting of the East European plate including the formation of the Kandalaksha graben (Artemieva, 2003; Bogdanova et al., 2008). Among Siberian xenoliths, only Grt-granulite Kom70 exhibits zircon resetting at 1656 ±27 Ma, post-dating the formation of the Kotuykan suture by 150-200 Myr.

Zircons from xenoliths from the southern margin of the Superior craton and the south Wyoming craton also recorded Mesoproterozoic extensional events (Zartman et al., 2012; Farmer et al., 2005). In Upper Michigan (Superior craton), migmatitic zircons have an age of 1.39 Ga that is interpreted as the response to intrusions of anorogenic granites. Later metamorphism at 1.1 Ga could be related to the Mid-Continent Rift flood basalt eruptions (Zartman et al., 2012).

The data on metamorphic zircons from mafic Grt-granulite xenoliths from beneath the Proterozoic Cheyenne belt are insufficient. Therefore, we have taken the youngest dates (1.38-1.34 Ga) as the age of granulite-facies association, although the presence of older metamorphic zircon generation is probable. Farmer et al. (2005) related the metamorphic event at 1.4-1.3 Ga to local granitoid plutonism.

Metamorphic zircons from both felsic and mafic Grt-granulite xenoliths from the Proterozoic Yavapai and Mazatzal orogenic provinces have ages of 1.42-1.38 Ga. Crowley et al. (2006) suggested that the granulite-facies metamorphism was due to anorogenic magmatism at 1.4 Ga.

4.3. Thermal history of the lower crust

According to heat flow data, the present-day temperature at the base of the crust in Precambrian areas is around 400-500 ^{o}C (e.g., Artemieva, 2003). U-Pb rutile age data record the time at which this state was reached (Schmitz and Bowring, 2003). Blackburn et al. (2011) examined the partial retention of Pb in rutile in xenoliths from the Medicine Hat block after a thermal disturbance and under conditions of slow cooling. They showed that the shallowest xenolith cooled below ~500^{o}C at about 1.8 Ga, around the time of metamorphic

zircon formation in upper crustal rocks. A Grt-gneiss xenolith from greater depth had cooled by 1.5 Ga, and the lower crustal Grt-granulite xenolith by 1.0 Ga. Blackburn et al. (2011) concluded that the data correspond better to a model of slow cooling (at the rate of <0.25^{o}C/Ma over ~500 Ma) than to reheating.

Davis et al. (2003) and Förster et al. (2017) obtained similar results of rutile U-Pb dating in xenoliths from the Slave craton. They demonstrated that mafic Grt-granulites cooled below the blocking temperature for Pb diffusion in rutile in the Mesoproterozoic (1388-1058 Ma). The latter values are broadly coincident with the intrusion of the 1.27 Ga giant Mackenzie dike swarm, suggesting reheating of the lower crust above the rutile closure temperature.

Xenoliths from the Belomorian mobile belt allow us to evaluate approximately the cooling rate after a re-heating event. If we assume that the peak temperature during the last granulite-facies event at 1640 Ma (U–Pb zircon age) was c. 900^{o}C (Zr-in rutile thermometer), and at 1560 Ma (Sm-Nd age of Grt-Cpx pair) the temperature was around 600^{o}C, which is close to the estimates for rims of garnet and clinopyroxene grains, then the cooling rate was about 4^{o}/Myr (Koreshkova et al., 2017) (Fig 6a). Scherer et al. (2000) estimated an average cooling rate between the 1707 Ma metamorphism (U–Pb zircon age) and the 1363 Ma Sm–Nd “closure” in Grt-clinopyroxenite xenolith from GFTZ as 0.75^{o}/Myr (Fig 6b). A cooling rate of 1-2^{o}/Myr was estimated in lower crustal xenoliths from the Mesoproterozoic Namaquan orogenic belt in Southern Africa (Schmitz and Bowring, 2003). The local lower crust was not disturbed until kimberlite eruptions that supports the robustness of the estimate. These estimates and that of Blackburn et al. (2011) point to a slow cooling in the lower crust, at the rate of ≤4^{o}/Myr.

Sm-Nd ages of garnet-clinopyroxene pairs from xenoliths are generally >100 Ma younger than Sm-Nd mineral isochrons ages of upper crustal rocks from the same region. For example, xenoliths of upper-middle crustal Grt-Bt-schists in Siberian kimberlites (the Alakit field) give ages from 1880 to 1840 Ma (Rosen et al., 2006), whereas lower crustal granulite xenoliths retained ages of 1750-920 Ma (Grt-Cpx pairs) (Buzlukova et al., 2006). A similar age difference is also observed in the Belomorian mobile belt and the Karelian craton (Kempton et al., 2001; Koreshkova et al., 2017; Peltonen et al., 2006), and at the southern margin of the Wyoming craton (Zartman et al., 2012). These data show that temperatures above ~600^{o}C lasted longer in the lower crust than in the middle-upper crust, assuming that the same thermal event affected both the lower and upper-middle crust. These data may also reflect reheating of the lower crust that occurred after lithospheric stabilization, i.e., during Mesoproterozoic events discussed in previous sections.

Some examples of correlation between zircon formation in the lower crust and metamorphism in the upper crust deserve detailed consideration. Since the metamorphic ages of 2.55-2.51 Ga in mafic Grt-granulite xenoliths from the Slave craton are younger than post-tectonic granitoids, Davis et al. (2003) pointed to a possibility of continued plastic flow in the lower crust that could trigger recrystallization of zircon grains. The data for xenoliths from the Bearpaw Mountains and the Sweetgrass Hills show that the formation of zircons in lower crustal rocks corresponds to late stages of metamorphism in the Great Falls Tectonic Zone followed by a slow cooling (Fig. 6b). Lower crustal xenoliths also reveal a possible reheating at ~1.3 Ga that may be linked to magmatism in the Belt Basin rift system (Barnhart et al., 2012; Mueller and Frost, 2006).

Another example of the correspondence of thermal events in both the upper and lower crust comes from the Belomorian mobile belt in NW Russia. In the lower crustal

xenoliths, metamorphic zircon generations older than 1.85 Ga may be related to regional events in the upper crust during the Lapland-Kola orogeny (Fig. 6a, 7a). Zircons with ages between 1.85 and 1.76 Ga could have formed during collision and extensional events during this period. The end of the orogeny was marked by the intrusion of A-type granites at 1.80-1.76 Ga (Daly et al., 2006). Younger zircons (<1.76 Ga) in lower crustal rocks were formed during several extensional events that were responsible for intrusion of lamprophyres and formation of the Kandalaksha graben (Bogdanova et al., 2008).

Figs. 6a, b. 1.5-column fitting image

However, there is no exact correspondence between the upper crustal events and zircon ages from xenoliths, as seen in Fig. 7a. Zircon formation at 1.86-1.81 Ga (average 1.83 Ga) in the lower crust may correspond to the latest migmatization stage within the Belomorian mobile belt (1875-1840 Ma (Bibikova et al., 2004)). Zircons dated at 1.73-1.77 Ga (average 1.75 Ga) may be compared to the 1.80-1.76 Ga post-tectonic granites. In both cases, however, zircons from xenoliths are somewhat younger. The shift to younger ages in the lower crust may be due to (a) limited data on xenoliths and poor preservation of older zircons or (b) different thermal histories of the upper and lower crust. The Belomorian mobile belt was the footwall of the Lapland-Kola orogen where uplift and cooling were delayed compared with the Lapland granulite belt (Daly et al., 2006). We assume that high-temperature conditions persisted even longer in the lower crust of the Belomorian mobile belt.

Probably, when the number of determinations is limited, partial resetting of older zircons during superimposed events can affect the age distribution. This may be the case for xenoliths from the Belomorian mobile belt. Nevertheless, similar difference in the ages of zircons from the upper and lower crustal rocks is observed in xenoliths from the Daldyn and Alakit kimberlite fields in Siberia. This is the most representative xenolith suite

comprising 25 lower crustal Grt-granulites and 16 upper-middle crustal gneisses and amphibolites. The age histogram (Fig. 7b) demonstrates that zircon ages in lower crustal rocks are generally younger than those in upper-middle crustal rocks, with maxima at 1.85 and 1.87-1.89 Ga, respectively. In the lower crust, the maximum coincides with the intrusion of post-tectonic granites (Rosen et al., 2006), although there is some displacement to younger ages.

Figs. 7a, b. 1-column fitting image

With slow cooling, a rejuvenation of zircon age due to volume diffusion of Pb is possible, if we take into account probable episodes of re-heating. As shown by Watson and Cherniak (2013), significant Pb-loss occurs during heating in addition to the loss during cooling. Prograde "diffusive opening" for Pb would start at 730°C for grain sizes of 50 μm and a cooling rate of 4°/Myr. Complete opening would be achieved at T>960°C which is similar to the closure temperature of 940°C (Dodson, 1973). However, no less likely, slow cooling and retention of high-temperature conditions can delay the net transfer formation of metamorphic zircons and promote dislocation creep that may cause recrystallization of existing zircons.

In the above examples, reheating events at ~1.3 Ga occurred after significant cooling of the lower crust that follows from Sm-Nd data for garnets and clinopyroxenes (Fig. 6a, b). There is no contradiction if take into account that in the eclogite xenolith Mk284, zircon was formed by exsolution from rutile, i.e., later than garnet and clinopyroxene. The Sm-Nd data are from Grt-granulite xenoliths, which are coarse-grained rocks. If a reheating event lasted 10-20 Ma or less, garnets and clinopyroxenes may have retained their isotopic compositions. Actually, seven xenoliths show Sm-Nd ages of garnet-clinopyroxene pairs within 1.61-1.54 Ga, but one Grt-granulite xenolith (Mk100) has an age of 1.33 Ga (Koreshkova et al., 2001). This shows the varying degree of reworking of lower crustal rocks

at that time. A similar explanation may apply to the Grt-clinopyroxenite xenolith RRE5a (Scherer et al., 2000).

The above considerations indicate that zircon ages in xenoliths may not reflect peak temperature conditions and that the formation of zircons in lower crustal rocks may be delayed relative to events recorded in the upper crust. However, the data from xenoliths from the Nakyn field in Siberia cannot be explained this way. Metamorphic zircon generation in upper crustal plagiogneiss Nur26 was formed 0.9 Ga earlier than in the lower crustal granulites (Table 1, ESM 1). The possible explanation why this upper crustal rock was not affected by thermal events around 1.9-1.8 Ga is that the lower crustal xenoliths came from a Proterozoic shear zone within the Archaean crust.

In summary, the major differences between metamorphic histories of the lower and upper crust are the slow cooling and long duration of thermal events in the lower crust. This may cause a delay in the formation of zircon and a resetting of earlier zircon generations in lower crustal rocks that explains the shift to younger ages.

4.4. The age of the lower crust of the Columbia supercontinent

Xenolith suites from Michigan and Siberia comprise rocks of Fe-rich tholeiitic composition (Koreshkova et al., 2011; Zartman et al., 2012) that implies that their parental melts fractionated at shallow depths, less than 0.7-0.8 GPa (Villiger et al., 2007). These rocks, and a few metasedimentary xenoliths from NW Russia (Koreshkova et al., 2014), Canada (Antonelli et al., 2019; Aulbach et al., 2020) and Michigan (Zartman et al., 2012), point to tectonic transport of material from the surface to the lower crust. Therefore, various processes led to the present assemblage of lower crustal rocks, including tectonic transport,

underplating of mantle magmas, and intracrustal melting. Consequently, the age of magmatic zircons cannot be regarded as the age of the lower crust in its present form.

The age of formation of the observed granulite-facies mineral association provides the minimum time limit when various components had assembled at lower crustal depths. This age can be inferred from data on metamorphic zircons in equilibrium with the observed mineral associations. An alternative way to obtain the age of the lower crust in its current form is to estimate the time when lower crustal rocks lost heat-producing elements. The lower continental crust in general is poor in heat-producing elements (Rudnick and Gao, 2003) that is widely recognized as the result of extraction of partial melts during amphibolite- to granulite-facies metamorphism. The removal of these elements from the lower crust is a condition for the formation of stable continental crust (e.g., Bolhar et al., 2007; Antonelli et al., 2019).

Bolhar et al. (2007) showed that Pb isotopic compositions of xenoliths from the Bearpaw Mountains in the northern Wyoming Craton correspond to a two-stage model: formation of protoliths in the Archaean and high-grade metamorphism and loss of U and Th in the Paleoproterozoic (2.1-1.6 Ga ago). Antonelli et al. (2019) studied Ca isotopic compositions of metamorphic rocks from several localities including four Grt-granulite xenoliths from the central Slave craton. They showed that these granulites lost a significant amount of K (~60-95 %) during high temperature metamorphism at about 2.5 Ga. These estimates are consistent with the U-Pb ages of metamorphic zircons from lower crustal xenoliths.

In our compilation, several localities demonstrate a multi-stage metamorphic history (Table 1, ESM 1). When the information about the relationship of zircon to the observed granulite-facies mineral association is not available, the minimum zircon age is

taken as the age of formation of the association. In summary, the lower crust of the Slave craton was formed 2.60-2.51 Ga ago, as confirmed by the age of titanite. The lower crust of the central Superior craton has an age of 2.58-2.42 Ga. The relationship of metamorphic zircons to the observed association is confirmed by mineral inclusions in them. In the Great Falls Tectonic Zone and northern Wyoming craton, the observed granulite-facies mineral associations were formed much later (1.79-1.71 Ga ago). The lower crust of the southern margin of the Superior craton was reworked and possibly underplated at 1.10 Ga due to the eruption of flood basalts of the Midcontinent Rift. The lower crust of the southern Wyoming craton was probably reworked about the same time but this is uncertain, as there is only one metamorphic zircon age determination. The lower crust of the Proterozoic Cheyenne belt and Yavapai and Mazatzal provinces was significantly reworked in the period of 1.43-1.38 Ga, during anorogenic magmatism (Fig. 1).

The lower crust of the Anabar province of the Siberian craton was formed between 1.88 and 1.78 Ga that follows from the age of metamorphic zircons equilibrated with the observed garnets (see sections 2.1, 3.3.1-3.3.4 for explanation). Moyen et al. (2017) came to a similar conclusion that Siberian lower crust is Paleoproterozoic, while Shatsky et al. (2019) claimed it was formed in the Archean. We emphasize that the material that composed the lower crust (the protoliths of granulites) is Archaean in age and was not replaced with Paleoproterozoic material since no Proterozoic magmatic zircons have been found so far. But the age of the lower crust as a lithospheric unit is Paleoproterozoic.

The Karelian lower crust has an age of 1.86-1.72 Ga. The lower crust of the Belomorian mobile belt was reworked at 1.65 Ga and, to a lesser extent, later in the Mesoproterozoic. However, these events did not erase the evidence of older metamorphism. The observed granulite-facies mineral associations were formed at 1.76 Ga and 1.84-1.81 Ga,

which follows from the trace element compositions of co-existing zircons and garnets and mineral inclusions in zircon.

We hope that further investigations will improve this picture. We expect more evidence of Archean metamorphism to be found in the lower crust of Archean cratonic areas. In particular, there are as yet no reported zircon ages for lower crustal xenoliths from the Hearne, Aldan, Rae or Nain provinces of the Columbia supercontinent (Fig. 1), which we would predict to show Archean magmatic and mostly Paleoproterozoic metamorphic ages.

5. Conclusion

Magmatic zircons from Archean cratonic areas that formed the central part of the Columbia supercontinent (the Slave, Wyoming, Superior, Siberian (Anabar province) and Karelian cratons, and the Belomorian mobile belt in NW Russia) have predominantly Archean ages (3.5-2.6 Ga). Addition of Proterozoic material may have occurred at craton boundaries and in areas of crustal extension. However, only three zircon samples with ages of 2.50-2.47 and 1.64 Ga have been reported. Therefore, no significant replacement with juvenile Proterozoic rocks took place in the lower crust.

Metamorphic zircons show a wide spread of ages from 2.6 to 1.1 Ga. These ages mean that the protoliths of different origin and age, including metasedimentary rocks or pre-existing lower crustal rocks, were assembled by this time at lower crustal depth and transformed into the present-day zircon-bearing associations. The granulite-facies associations formed in the Archean have been preserved in lower crustal rocks of the Slave and Superior cratons despite later re-heating events. In xenoliths from the Wyoming, Siberian and Karelian cratons, and the Belomorian mobile belt, the formation of high-pressure

granulite-facies associations occurred predominantly in the period of 1.9-1.7 Ga during the Proterozoic orogenic events that assembled the Columbia supercontinent. These xenolith localities are situated near the boundaries with Proterozoic orogenic belts where tectonic burial and sub-horizontal movements of rock complexes took place. Nevertheless, sporadic metamorphic zircons survived the orogenic events that shows the probability of preservation of Archean lower crust remnants.

After lithospheric stabilization, the lower crust of Columbia experienced several reheating events that caused formation of new granulite-facies associations and subsolidus zircon growth. In the Belomorian mobile belt, multiple episodes of reheating occurred over the period of 1.67-1.27 Ga with weak manifestation of related magmatism at the surface. Extensional events and related magmatism at 1.4 and 1.1 Ga at the southern margin of the Superior craton caused significant reworking of the lower crust with migmatization and formation of granulite-facies associations. Whereas in the Slave craton, which was largely affected by the Mackenzie plume (1.27 Ga), it mostly caused resetting of rutile ages.

In Proterozoic orogenic belts, lower crustal rocks have protolith ages that coincide with those in juvenile upper crustal rocks. Samples from the Yavapai and Mazatzal provinces and the Cheyenne belt demonstrate reworking with the formation of granulite-facies associations during anorogenic magmatism at around 1.4 Ga. However, the preservation of 1.7-1.6 Ga old metamorphic zircons is probable in xenoliths from the Cheyenne belt.

We take the age of the lower crust as the age of the observed association, which is dated by zircon equilibrated with garnet. Thus, the granulitic lower crust of the central part of the Columbia supercontinent was formed in the Proterozoic, mainly in the

period of 1.9-1.7 Ga. A few regions preserved the Archean granulitic lower crust (Fig. 1). The major differences between metamorphic histories of the lower and upper crust are the slow cooling and long duration of thermal events in the lower crust.

Acknowledgements

We thank Dr Martin Rittner and Dr Andy Beard (Birkbeck) for technical help with laser probe analyses, and Dr Aleksandr Larionov (Vsegei, St Petersburg) for discussion of geochronological data.

References

Antonelli, M.A., DePaolo, D.J., Chacko, T., Grew, E.S., Rubatto, D., 2019. Radiogenic Ca isotopes confirm post-formation K depletion of lower crust. Geochemical Perspectives Letters 9, 43-48. https://doi.org/10.7185/geochemlet.1904

Artemieva, I.M., 2003. Lithospheric structure, composition, and thermal regime of the East European craton: implications for the subsidence of the Russian platform. Earth and Planetary Science Letters 213, 431–446. https://doi.org/10.1016/S0012-821X(03)00327-3

Aulbach, S., Krauss, C., Creaser, R.A., Stachel, T., Heaman, L.M., Matveev, S., Chacko, T., 2010. Granulite Sulphides as Tracers of Lower Crustal Origin and Evolution: An Example from the Slave craton, Canada. Geochimica et Cosmochimica Acta 74, 5368-5381. https://doi.org/10.1016/j.gca.2019.05.044

Aulbach S., Symes C., Chacko, T., 2020. Elemental and radiogenic isotope perspective on formation and transformation of cratonic lower crust: Central Slave craton (Canada).

Geochimica et Cosmochimica Acta 278, 78-93. https://doi.org/10.1016/j.gca.2010.06.005

Balagansky V., Shchipansky, A., Slabunov, A., Gorbunov, I., Mudruk, S., Sidorov, M., Azimov, P., Egorova, S., Stepanova, A., Voloshin, A., 2015. Archaean Kuru-Vaara eclogites in the northern Belomorian Province, Fennoscandian Shield: crustal architecture, timing, and tectonic implications. International Geology Review 57, 1543-1565. https://doi.org/10.1016/S0012-821X(03)00327-3

Barnhart, K.R., Mahan, K.H., Blackburn, T.J., Bowring, S.A., Dudas, F.O., 2012. Deep crustal xenoliths from central Montana, USA: implications for the timing and mechanisms of high-velocity lower crust formation. Geosphere 8, 1408–1428. https://doi.org/10.1130/GES00765.1

Bibikova, E., Skiöld, T., Bogdanova, S., Gorbatschev, R., Slabunov, A., 2001. Titanite-rutile thermochronometry across the boundary between the Archaean Craton in Karelia and the Belomorian Mobile Belt, eastern Baltic Shield. Precambrian Research 105, 315–330. https://doi.org/10.1016/S0301-9268(00)00117-0

Bibikova, E.V., Bogdanova, S.V., Glebovitsky, V.A., Claesson, S., Skiöld, T., 2004. Evolution of the Belomorian Belt: NORDSIM UPb Zircon Dating of the Chupa Paragneisses, Magmatism, and Metamorphic Stages. Petrology 12, 195-210.

Blackburn, T., Bowring, S.A., Schoene, B., Mahan, K., Dudas, F., 2011. U-Pb thermochronology: creating a temporal record of lithosphere thermal evolution. Contributions to Mineralogy and Petrology 162, 479–500. https://doi.org/10.1007/s00410-011-0607-6

Bloch, E., Ganguly, J., Hervig, R., Cheng, W., 2015. ^{176}Lu–^{176}Hf geochronology of garnet I: experimental determination of the diffusion kinetics of Lu^{3+} and Hf^{4+} in garnet, closure temperatures and geochronological implications. Contributions to Mineralogy and Petrology169, 12. https://doi.org/10.1007/s00410-015-1109-8

Bogdanova, S.V., Bingen, B., Gorbatschev, R., Kheraskova, T.N., Kozlov, V.I., Puchkov, V.N., Volozh, Yu.A., 2008. The East European Craton (Baltica) before and during the assembly of Rodinia. Precambrian Research 160, 23-45. https://doi.org/10.1016/j.precamres.2007.04.024

Bolhar, R., Kamber, B.S., Collerson, K.D., 2007. U-Th-Pb fractionation in Archaean lower continental crust: Implications for terrestrial Pb isotope systematics. Earth and Planetary Science Letters 254, 127-145. https://doi.org/10.1016/j.epsl.2006.11.032

Burnham, A.D., Berry, A.J., 2012. An experimental study of trace element partitioning between zircon and melt as a function of oxygen fugacity. Geochimica et Cosmochimica Acta 95, 196–212. https://doi.org/10.1016/j.gca.2012.07.034

Buzlukova, L.V., Shatsky, V.S., Sobolev, N.V., 2004. Specific structure of the lowermost Earth's crust at the Zagadochnaya kimberlite pipe, Yakutia. Russian Geology and Geophysics 45, 992-1007.

Chen, Y., Gu, Y. G., Hung, S.-H., 2017. Finite-frequency P-wave tomography of the Western Canada Sedimentary Basin: Implications for the lithospheric evolution in Western Laurentia. Tectonophysics 698, 79–90. http://dx.doi.org/10.1016/j.tecto.2017.01.006

Cherniak, D.J., Watson, B.E., 2003. Diffusion in zircon. Reviews in Mineralogy and Geochemistry 53, 113–143.

Claesson, S., Vetrin, V., Bayanova, T., Downes, H., 2000. U–Pb zircon ages from a Devonian carbonatite dyke, Kola peninsula, Russia: a record of geological evolution from the Archaean to the Palaeozoic. Lithos 51, 95-108. https://doi.org/10.1016/S0024-4937(99)00076-6

Claiborne L.L., Miller, C.F., Gualda, G.A.R., Carley, T.L., Covey, A.K., Wooden, J.L., Fleming, M.A., 2018. Zircon as Magma Monitor: Robust, Temperature-Dependent Partition Coefficients from Glass and Zircon Surface and Rim Measurements from Natural Systems. In: Moser, D.E., Corfu, F., Darling, J.R., Reddy, S.M., Tait, K. (Eds.), Microstructural Geochronology: Planetary Records Down to Atom Scale, Geophysical Monograph 232, First Edition. John Wiley & Sons, Inc., Hoboken, and American Geophysical Union, Washigton, pp. 3-33.

Corfu, F., Hanchar, J.M., Hoskin, P.W.O., Kinny, P., 2003. Atlas of zircon textures. Reviews in Mineralogy and Geochemistry 53, 469-500.

Crowley, J.L., Schmitz, M.D., Bowring, S.A., Williams, M.L., Karlstrom, K.E., 2006. U–Pb and Hf isotopic analysis of zircon in lower crustal xenoliths from the Navajo volcanic field: 1.4 Ga mafic magmatism and metamorphism beneath the Colorado Plateau. Contributions to Mineralogy and Petrology 151, 313–330. https://doi.org/10.1007/s00410-006-0061-z

Daly, J.S., Balagansky, V.V., Timmerman, M.J., Whitehouse, M.J., 2006. The Lapland-Kola orogen: Palaeoproterozoic collision and accretion of the northern Fennoscandian lithosphere. Geological Society London Memoirs 32, 579-598. https://doi.org/10.1144/GSL.MEM.2006.032.01.35

Davis, J.W., Canil, D., MacKenzie, J.M., Carbno, G.B., 2003. Petrology and U-Pb geochronology of lower crustal xenoliths and the development of a craton, Slave Province, Canada. Lithos 71, 541-573. https://doi.org/ 10.1016/S0024-4937(03)00130-0

Dhuime, B., Bosch, D., Bodinier, J.-L., Garrido, C.J., Bruguier, O., Hussain, S.S., Dawood, H., 2007. Multistage evolution of the Jijal ultramafic-mafic complex (Kohistan, N Pakistan): Implications for building the roots of island arcs. Earth and Planetary Science Letters 261, 179–200. https://doi.org/10.1016/j.epsl.2007.06.026

Downes, H., Peltonen, P., Mänttäri, I., Sharkov, E.V., 2002. Proterozoic zircon ages from lower crustal granulite xenoliths, Kola Peninsula: evidence for crustal growth and reworking. Journal of the Geological Society London 159, 485–488. https://doi.org/10.1144/0016-764901-162

Evans, D.A.D., Mitchell, R.N., 2011. Assembly and breakup of the core of Paleoproterozoic-Mesoproterozoic supercontinent Nuna. Geology 39, 443–446. https://doi.org/10.1130/G31654.1

Ewing, T., Rubatto, D., Hermann, J., 2014. Hafnium isotopes and Zr/Hf of rutile and zircon from lower crustal metapelites (Ivrea–Verbano Zone, Italy): Implications for chemical differentiation of the crust. Earth and Planetary Science Letters 389, 106–118. https://doi.org/10.1016/j.epsl.2013.12.029

Farmer, G.L., Bowring, S.A., Williams, M.L., Christensen, N.I., Matzel, J., Stevens, L., 2005. Contrasting lower crustal evolution across an Archean–Proterozoic suture: physical, chemical and geochronologic studies of lower crustal xenoliths in southern Wyoming

and northern Colorado. In: Karlstrom, K.E., and Keller, G.R., (Eds.), The Rocky Mountain Region: an Evolving Lithosphere. American Geophysical Union, Washigton, 139-162. https://doi.org/10.1029/154GM11

Förster, B., Aulbach, S., Symes, C., Gerdes, A., Hofer, H.E., Chacko, T., 2017. A Reconnaissance Study of Ti-minerals in Cratonic Granulite Xenoliths and their Potential as Recorders of Lower Crust Formation and Evolution. Journal of Petrology 58, 2007-2034. https://doi.org/10.1093/petrology/egx080

Gauthiez-Putallaz, L., Rubatto, D., Hermann, J., 2016. Dating prograde fluid pulses during subduction by in situ U–Pb and oxygen isotope analysis. Contributions to Mineralogy and Petrology 171, 15. https://doi.org/10.1007/s00410-015-1226-4

Glebovitskii, V., Marker, M., Alexejev, N., Bridgwater, D., Sedova, I., Salnikova, E., Berezhnaya, N., 2001. Age, evolution and regional setting of the Palaeoproterozoic Umba igneous suite in the Kolvitsa-Umba zone, Kola Peninsula: constraints from new geological, geochemical and U-Pb zircon data. Precambrian Research 105, 247–267. https://doi.org/10.1016/S0301-9268(00)00114-5

Glebovitskii, V.A., Baltybaev, S.K., Levchenkov, O.A., Kuzmina, E.V., 2009. Thermodynamic regime of Svecofennian (1.9 Ga) metamorphism of the Umba nappe of the Lapland collisional orogen. Petrology 17, 331–351. https://doi.org/10.1134/S086959110904002X

Gorman, A.R., Clowes, R.M., Ellis, R.M., Henstock, T.J., Levander, A., Spence, G.D., Kanasewich, E.R., 2002. Deep Probe: imaging the roots of western North America. Canadian Journal of Earth Sciences 39, 375–398. https://doi.org/10.1139/e01-064

Grimes, C.B., Wooden, J.L., Cheadle, M.J., John, B.E., 2015. “Fingerprinting” tectono‐magmatic provenance using trace elements in igneous zircon. Contributions to Mineralogy and Petrology 170, 46. https://doi.org/10.1007/s00410-015-1199-3

Harms, T.A., Burger, H.R., Blednick, D.G., Cooper, J.M., King, J.T., Owen, D.R., Lowell, J., Sincock, M.J., Kranenburg, S.R., Pufall, A., Picornell, C.M., 2004. Character and origin of Precambrian fabrics and structures in the Tobacco Root Mountains, Montana. Geological Society of America Special Papers 377, 203–226. https://doi.org/10.1130/0-8137-2377-9.203

Heaman, L.M., Pearson, D.G., 2010. Nature and evolution of the Slave Province subcontinental lithospheric mantle. Canadian Journal of Earth Sciences 47, 369-388. https://doi.org/10.1139/E09-046

Helmstaedt, H., 2009. Crust-mantle coupling revisited: The Archean Slave craton, NWT, Canada. Lithos 112, 1055-1068. https://doi.org/10.1016/j.lithos.2009.04.046

Hölltä, P., Huhma, H., Mänttäri, I., Peltonen, P., Juhanoja, J., 2000. Petrology and geochemistry of mafic granulite xenoliths from the Lahtojoki kimberlite pipe, eastern Finland. Lithos 51, 109-133. https://doi.org/10.1016/S0024-4937(99)00077-8

Hoskin, P.W.O., Black, L.P., 2000. Metamorphic zircon formation by solid-state recrystallisation of protolith igneous zircon. Journal of Metamorphic Geology 18, 423–439. https://doi.org/10.1046/j.1525-1314.2000.00266.x

Hoskin, P.W.O., Schaltegger, U., 2003. The composition of zircon and igneous and metamorphic petrogenesis. Reviews in Mineralogy and Geochemistry 53, 27-62.

Kempton, P.D., Downes, H., Neymark, L.A., Wartho, J.A., Zartman, R.E., Sharkov, E.V., 2001. Garnet granulite xenoliths from the Northern Baltic Shield—the underplated lower crust of a Palaeoproterozoic large igneous province? Journal of Petrology 42, 731–763. https://doi.org/10.1093/petrology/42.4.731

Kohn, M.J., 2017. Titanite Petrochronology. Reviews in Mineralogy and Geochemistry 83, 419–441. https://doi.org/10.2138/rmg.2017.83.13

Koreshkova, M.Yu., Downes, H., Nikitina LP, Vladykin NV, Larionov AN, Sergeev SA (2009) Trace element and age characteristics of zircons in granulite xenoliths from the Udachnaya kimberlite pipe, Siberia. Precambrian Research 168, 197–212. https://doi.org/10.1016/j.precamres.2008.09.007

Koreshkova, M.Yu., Downes, H., Levsky, L.K., Vladykin, N.V., 2011. Petrology and geochemistry of granulite xenoliths from Udachnaya and Komsomolskaya kimberlite pipes, Siberia. Journal of Petrology 52, 1857–1885. https://doi.org/10.1093/petrology/egr033

Koreshkova, M.Yu., Downes, H., Glebovitsky, V.A., Rodionov, N.V., Antonov, A.V., Sergeev, S.A., 2014. Zircon trace element characteristics and ages in granulite xenoliths: a key to understanding the age and origin of the lower crust, Arkhangelsk kimberlite province, Russia. Contributions to Mineralogy and Petrology 167, 973. https://doi.org/10.1007/s00410-014-0973-y

Koreshkova, M., Downes, H., Millar, I., Levsky, L., Larionov, A., Sergeev, S., 2017. Geochronology of Metamorphic Events in the Lower Crust beneath NW Russia: a

Xenolith Hf Isotope Study. Journal of Petrology 58, 1567-1590. https://doi.org/10.1093/petrology/egx065

Koreshkova, M.Yu., Levsky, L.K., Ivanikov, V.V., 2001. Petrology of a lower crustal xenolith suite from dykes and explosion pipes of Kandalaksha graben. Petrology 9, 79–96.

Kostrovitsky, S.I., Skuzovatov, S.Yu., Yakovlev, D.A., Sun, J., Nasdala, L., Wu, F., 2016. Age of the Siberian craton crust beneath the northern kimberlite fields: insights to the craton evolution. Gondwana Research 39, 365–385. https://doi.org/10.1016/j.precamres.2019.105388

Kovaleva, E., Klötzli, U., Habler, G., Libowitzky, E., 2014. Finite lattice distortion patterns in plastically deformed zircon grains. Solid Earth, 5, 1099–1122. https://doi.org/10.5194/se-5-1099-2014

Kuusisto, M., Kukkonen, I.T., Heikkinen, P., Pesonen, L.J., 2006. Lithological interpretation of crustal composition in the Fennoscandian Shield with seismic velocity data. Tectonophysics 420, 283–299. https://doi.org/10.1016/j.tecto.2006.01.014

Lee, C.-T.A., Cheng, X., Horodyskyj. U., 2006. The development and refinement of continental arcs by primary basaltic magmatism, garnet pyroxenite accumulation, basaltic recharge and delamination: insights from the Sierra Nevada, California. Contributions to Mineralogy and Petrology 151, 222–242. https://doi.org/10.1007/s00410-005-0056-1

Levskii, L.K., Morozova, I.M., Savatenkov, V.M., 2003. Isotope Geothermometers: Applications and Limitations. Petrology 11, 352-364.

Liu, Y.S., Gao, S., Jin, S.Y., Hu, S.H., Sun, M., Zhao, Z.B., Feng, J.L., 2001. Geochemistry of lower crustal xenoliths from Neogene Hannuoba Basalt, North China Craton: Implications for petrogenesis and lower crustal composition. Geochimica et Cosmochimica Acta 65 (15), 2589–2604. https://doi.org/10.1016/S0016-7037(01)00609-3

Loucks, R.R., Fiorentini, M.L., Rohrlach, B.D., 2018. Divergent T–fO_2 paths during crystallisation of H_2O-rich and H_2O-poor magmas as recorded by Ce and U in zircon, with implications for TitaniQ and TitaniZ geothermometry. Contributions to Mineralogy and Petrology 173, 104. https://doi.org/ 10.1007/s00410-018-1529-3

Markwick, A.J.W., Downes, H., Veretennikov, N., 2001. The lower crust of SE Belarus: petrological, geophysical and geochemical constraints from xenoliths. Tectonophysics 339, 215-237. https://doi.org/10.1016/S0040-1951(01)00040-3

Meert, G.J., 2012. What's in a name? The Columbia (Paleopangaea/Nuna) supercontinent. Gondwana Research 21, 987–993. https://doi.org/10.1016/j.gr.2011.12.002

Meert, G.J., Santosh, M., 2017. The Columbia supercontinent revisited. Gondwana Research 50, 67–83. https://doi.org/10.1016/j.gr.2017.04.011

Mintz, M.V., Dokukina, K.A., Konilov, A.N., 2014. The Meso-Neoarchaean Belomorian eclogite province: Tectonic position and geodynamic evolution. Gondwana Research 25, 561–584. http://dx.doi.org/10.1016/j.gr.2012.11.010

Mintz, M.V., Kaulina, T.V., Konilov, A.N., Krotov, A.V., Stupak, V.M., 2007. The thermal and geodynamic evolution of the Lapland granulite belt: Implications for thermal

structure of the lower crust during granulite-facies metamorphism. Gondwana Research 12, 252–267. https://doi.org/10.1016/j.gr.2006.10.007

Mirnejad, H., Bell, K., 2008. Geochemistry of Crustal Xenoliths from the Hatcher Mesa Lamproite, Wyoming, USA: Insights into the Composition of the Deep Crust and Upper Mantle beneath the Wyoming Craton. Canadian Mineralogist 46, 583-596. https://doi.org/10.3749/canmin.46.3.583

Moser, D.E., Heaman, L.M., 1997. Proterozoic zircon growth in Archean lower crustal xenoliths, southern Superior craton – a consequence of Matachewan ocean opening. Contributions to Mineralogy and Petrology 128, 164-175. https://doi.org/10.1007/s004100050301

Moyen, J.-F., Paquette, J.L., Ionov, D.A., Gannoun, A., Korsakov, A.V., Golovin, A.V., Moine, B.N., 2017. Paleoproterozoic rejuvenation and replacement of Archaean lithosphere: evidence from zircon U-Pb dating and Hf isotopes in crustal xenoliths at Udachnaya, Siberian craton. Earth and Planetary Science Letters 457, 149–159. https://doi.org/10.1016/j.epsl.2016.09.046

Mueller, P., Frost, C., 2006. The Wyoming Province: A distinctive Archean craton in Laurentian North America. Canadian Journal of Earth Sciences 43, 1391–1397. https://doi.org/10.1139/e06-075.

Nikitina, L.P., Levskii, L.K., Lokhov, K.I., Belyatskii, B.V., Zhuravlev, V.A., Lepekhina, E.V., Antonov, A.V., 1999. Proterozoic alkaline ultramafic magmatism in the eastern part of the Baltic Shield. Petrology 7, 246-266.

Nance, R.D., Murphy, J.B., Santosh, M., 2014. The supercontinent cycle: a retrospective essay. Gondwana Research, 25, 4–29. http://dx.doi.org/10.1016/j.gr.2012.12.026

Nironen, M., 2017. Guide to the Geological Map of Finland – Bedrock 1:1 000 000. Geological Survey of Finland, Special Paper 60, 41-76.

Peltonen, P., Mänttäri, I., Huhma, H., Whitehouse, M.J., 2006. Multi-stage origin of the lower crust of the Karelian craton from 3.5 to 1.7 Ga based on isotopic ages of kimberlite-derived mafic granulite xenoliths. Precambrian Research 147, 107–123. https://doi.org/10.1016/j.precamres.2006.02.008

Percival, J.A., Skulski, T., Sanborn-Barrie, M., Stott, G.M., Leclair, A.D., Corkery, M.T., Boily, M., 2012. Geology and tectonic evolution of the Superior Province, Canada, in: Percival, J.A., Cook, F.A., Clowes, R.M., (Eds), Tectonic Styles in Canada: The LITHOPROBE Perspective. Geological Association of Canada, Special Paper 49, 321–378. ISBN: 978-1-897095-60-7

Pesonen, L.J., Mertanen, S., Veikkolainen, T., 2012. Paleo-Mesoproterozoic Supercontinents - A Paleomagnetic View. Geophysica 47, 3–46.

Pisarevsky, S.A., Natapov, L.M., Donskaya, T.V., Gladkochub, D.P., Vernikovsky, D.A., 2008. Proterozoic Siberia: A promontory of Rodinia. Precambrian Research 160, 66-76. https://doi.org/10.1016/j.precamres.2007.04.016

Poirier, J.-P., 1985. Creep of crystals. Cambridge University Press, Cambridge, London, New York, New Rochelle, Melbourne, Sydney. https://doi.org/10.1017/S0016756800035664

Reddy, S.M., Timms, N.E., Trimby, P., Kinny, P.D., Buchan, C., Blake, K., 2006. Crystal-plastic deformation of zircon: A defect in the assumption of chemical robustness. Geology 34, 257–260. https://doi.org/10.1130/G22110.1

Rogers, J.J., Santosh, M., 2002. Configuration of Columbia, a Mesoproterozoic supercontinent. Gondwana Research 5, 5–22. https://doi.org/10.1016/S1342-937X(05)70883-2

Rosen, O.M., Levsky, L.K., Zhuravlev, D.Z., Rotman, A.Ya., Spetsius, Z.V., Makeev, A.F., Zinchuk, N.N., Manakov, A.V., Serenko, V.P., 2006. Paleoproterozoic accretion in the northeast Siberian craton: isotopic dating of the Anabar collision system. Stratigraphy and Geological Correlation 14, 581-601. https://doi.org/10.1134/S0869593806060013

Rubatto, D., Hermann, J., 2007. Experimental zircon/melt and zircon/garnet trace element partitioning and implications for the geochronology of crustal rocks. Chemical Geology 241, 38–61. https://doi.org/10.1016/j.chemgeo.2007.01.027

Rubatto, D., 2017. Zircon: The Metamorphic Mineral. Reviews in Mineralogy and Geochemistry 83, 261–295. https://doi.org/10.2138/rmg.2017.83.9

Rudnick, R.L., Gao, S., 2003. Composition of the continental crust. In: Holland, H.D., Turekian, K.K. (Eds.), Treatise on Geochemistry. Elsevier, Amsterdam, 1-64. https://doi.org/10.1016/B0-08-043751-6/03016-4

Rumpfhube, E.-M., Keller, G.R., 2009. An integrated analysis of controlled and passive source seismic data across an Archean-Proterozoic suture zone in the Rocky

Mountains. Journal of Geophysical Research 114, B08305. https://doi.org/10.1029/2008JB005886

Schaltegger, U., Fanning, C.M., Gunther, D., Maurin, J.C., Schulmann, K., Gebauer, D., 1999. Growth, annealing and recrystallization of zircon and preservation of monazite in high-grade metamorphism: conventional and in-situ U-Pb isotope, cathodoluminescence and microchemical evidence. Contributions to Mineralogy and Petrology 134, 186-201. https://doi.org/10.1007/s004100050478

Schaltegger, U., Schmitt, A.K., Horstwood, M.S.A., 2015. U–Th–Pb zircon geochronology by ID-TIMS, SIMS, and laser ablation ICP-MS: Recipes, interpretations, and opportunities. Chemical Geology 402, 89-110. http://dx.doi.org/10.1016/j.chemgeo.2015.02.028

Scherer, E.E., Cameron, K.L., Blichert-Toft, J., 2000. Lu–Hf garnet geochronology: Closure temperature relative to the Sm–Nd system and the effects of trace mineral inclusions. Geochimica et Cosmochimica Acta 64, 3413–3432. https://doi.org/10.1016/S0016-7037(00)00440-3

Schmitz, M.D., Bowring, S.A., 2003. Constraints on the thermal evolution of continental lithosphere from U-Pb accessory mineral thermochronometry of lower crustal xenoliths, southern Africa. Contributions to Mineralogy and Petrology 144, 592–618. https://doi.org/10.1007/s00410-002-0419-9

Selverstone, J., Pun, A., Condie, K.C., 1999. Xenolithic evidence for Proterozoic crustal evolution beneath the Colorado Plateau. Geological Society of America Bulletin 111, 590–606. https://doi.org/10.1130/0016-7606(1999)111<0590:XEFPCE>2.3.CO;2

Shatsky, V.S., Malkovets, V.G., Belousova, E.A., Tretiakova, I.G., Griffin, W.L., Ragozin, A.L., Gibsher, A.A., O'Reilly, S.Y., 2016. Tectonothermal evolution of the continental crust beneath the Yakutian diamondiferous province (Siberian craton): U-Pb and Hf isotopic evidence on zircons from crustal xenoliths of kimberlite pipes. Precambrian Research 282, 1–20. https://doi.org/10.1016/j.precamres.2016.06.022

Shatsky, V.S., Malkovets, V.G., Belousova, E.A., Tretiakova, I.G., Griffin, W.L., Wang, Q., Ragozin, A.L., Gibsher, A.A., O'Reilly, S.Y., 2018. Multi-stage modification of Paleoarchean crust beneath the Anabar tectonic province (Siberian craton). Precambrian Research 305, 125–144. https://doi.org/10.1016/j.precamres.2017.11.017

Shatsky, V.S., Wang, Q., Skuzovatov, S.Yu., Ragozin, A.L., 2019. The crust-mantle evolution of the Anabar tectonic province in the Siberian Craton: Coupled or decoupled? Precambrian Research 332, 105388. https://doi.org/10.1016/j.precamres.2019.105388

Sláma, J., Košler, J., Pedersen, R.B., 2007. Behaviour of zircon in high-grade metamorphic rocks: Evidence from Hf isotopes, trace elements and textural studies. Contributions to Mineralogy and Petrology 154, 335–356. https://doi.org/10.1007/s00410-007-0196-6

Su, Y.P., Zheng, J.P., Griffin, W.L., Huang, Y., Wei, Y., Ping X., 2017. Geochronology and geochemistry of deep-seated crustal xenoliths in the northern North China Craton: Implications for the evolution and structure of the lower crust. Lithos 292–293, 1–14 https://doi.org/10.1016/j.lithos.2017.08.017

Taylor, R.J.M., Harley, S.L., Hinton, R.W., Elphick, S., Clark, C., Kelly, N.M., 2014. Experimental determination of REE partition coefficients between zircon, garnet and melt: A key to understanding high-T crustal processes. Journal of Metamorphic Geology 33, 231–248. https://doi.org/10.1111/jmg.12118

Thakurdin, Y., Bolhar, R., Horváth, P., Rocholld, A., Collerson, K., 2019a. Characterization of crustal xenoliths from the Bearpaw Mountains, Montana (USA), using U-Pb geochronology, whole-rock geochemistry and thermobarometry, with implications for lower crustal processes and evolution of the Wyoming Craton. Chemical Geology 524, 295–322. https://doi.org/10.1016/j.chemgeo.2019.07.034

Thakurdin, Y., Bolhar, R., Horváth, P., Wiedenbeck, M., Rocholld, A., 2019b. Formation of lower to middle crust of the Wyoming Craton, Montana (USA), using evidence from zircon Hf-O isotopic and trace element compositions. Chemical Geology 525, 218–244. https://doi.org/10.1016/j.chemgeo.2019.07.021

Vervoort, J.D., Patchett, P.J., Albarède, F., Blichert-Toft, J., Rudnick, R., Downes, H., 2000. Hf–Nd isotopic evolution of the lower crust. Earth and Planetary Science Letters 181, 115–129. https://doi.org/10.1016/S0012-821X(00)00170-9

Vetrin, V.R., Lepekhina, E.N., Paderin, I.P., Rodionov, N.V., 2009. Stages of the Lower Crust Formation of the Belomorian Mobile Belt, Kola Peninsula. Doklady Earth Sciences 425, 269-273. https://doi.org/10.1134/S1028334X09020214

Vetrin, V.R., Belousova, E.A., Kremenetsky, A.A., 2009. Stages of the Lower Crust Formation of the Belomorian Mobile Belt, Kola Peninsula. Doklady Earth Sciences 425, 269-273. https://doi.org/10.1134/S1028334X09020214

Villiger, S., Ulmer, P., Müntener, O., Thompson, A. 2004. The Liquid Line of Descent of Anhydrous, Mantle-Derived, Tholeiitic Liquids by Fractional and Equilibrium Crystallization - an Experimental Study at 1.0 GPa. Journal of Petrology 45, 2369-2388. https://doi.org/10.1093/petrology/egh042

Watson, E.B., Cherniak, D.J., 2013. Simple equations for diffusion in response to heating. Chemical Geology 335, 93–104. https://doi.org/10.1016/j.chemgeo.2012.10.054

Wei, Y., Zheng, J.P., Su, Y.P., Ma, Q., Griffin, W.L., 2015. Lithological and age structure of the lower crust beneath the northern edge of the North China Craton: xenolith evidence. Lithos 216–217, 211–223. https://doi.org/10.1016/j.lithos.2014.12.014

Woodard, J., Kietäväinen, R., Eklund, O., 2014. Svecofennian post-collisional shoshonitic lamprophyres at the margin of the Karelia Craton: Implications for mantle metasomatism. Lithos 205, 379–393. https://doi.org/10.1016/j.lithos.2014.06.021

Zartman, R.E., Kempton, P.D., Paces, J.B., Downes, H., Williams, I.S., Dobosi, G., Futa, K., 2012. Lower-Crustal Xenoliths from Jurassic Kimberlite Diatremes, Upper Michigan (USA): Evidence for Proterozoic Orogenesis and Plume Magmatism in the Lower Crust of the Southern Superior Province. Journal of Petrology 54, 575-608. https://doi.org/10.1093/petrology/egs079

Zheng, J.P., Griffin, W.L., Qi, L., O'Reilly, S.Y., Sun, M., Zheng, S., Pearson, N., Gao, J.F., Yu, C.M., Su, Y.P., Tang, H.Y., Liu, Q.S., Wu, X.L., 2009. Age and composition of granulite and pyroxenite xenoliths in Hannuoba basalts reflect Paleogene underplating beneath the North China Craton. Chemical Geology 264, 266–280. https://doi.org/10.1016/j.chemgeo.2009.03.011

Marina Koreshkova is an Associated Professor of the Department of Petrology at the Institute of Earth Sciences, St Petersburg State University, St Petersburg, Russia. She studied at St Petersburg State University, where she defended her thesis in 2001. Research interests: igneous and metamorphic petrology, structural petrology, geochemistry, and geochronology. Her research work focuses on the origin and metamorphic history of the continental lower crust.

Hilary Downes is a Professor of Geochemistry at Birkbeck University of London. She studied at the University of Durham and the University of Leeds, where she obtained her PhD. She has research interests in the formation and evolution of the lithosphere.

Figure captions:

Figure 1. Scheme of localities of lower crustal xenoliths with the ages of formation of granulite-facies associations taken as the age of the lower crust. The reconstruction of the central part of the supercontinent at 1270 Ma is from Evans and Mitchell (2011). Light grey areas are Archean cratons, grey areas – Early Proterozoic orogens (>1.8 Ga), dark grey areas - Early Proterozoic-Mesoproterozoic orogens (1.8-1.1 Ga).

Figure 2. Internal texture and REE composition of different zircon generations from Grt-granulite xenolith (sample Y53) from the Udachnaya kimberlite pipe, Siberia. Dashed lines are calculated compositions of zircon in equilibrium with garnet from this sample using $D^{Zrn/Grt}$ from Rubatto and Hermann (2007). (In this sample, the difference in REE contents between zircon generations with homogeneous and convoluted textures is small. Both of them could have equilibrated with garnet at 900-950^{o}C.)

Figure 3. εHf(t) vs U–Pb zircon age in lower crustal xenoliths from Kola and Arkhangelsk regions, NW Russia (Koreshkova et al., 2017), the Bearpaw Mountains, Montana (Scherer et al., 2000; Thakurdin et al., 2019b), and the Colorado Plateau (Crowley et al., 2006). Dashed lines with corresponding sample numbers are Pb-loss trajectories. Solid lines are bulk-rock samples (Crowley et al., 2006; Koreshkova et al., 2017; Scherer et al., 2000). DM, Depleted Mantle; CHUR, Chondritic Uniform Reservoir. Uncertainty in εHf(t) is ~2ε. WR – whole rock composition.

Figure 4. εHf(t) vs U–Pb zircon age in lower crustal Grt-granulite xenoliths from the Alakit and Daldyn kimberlite fields, Siberia (Shatsky et al., 2016, 2018, 2019; Moyen et al., 2017). Dashed line is a Pb-loss trajectory for the oldest magmatic core from sample ZAR-3-05. Solid lines are bulk-rock samples: Uk1, Uk5, Uk37 and Y6 (Koreshkova et al., 2011). DM, Depleted Mantle; CHUR, Chondritic Uniform Reservoir. Uncertainty in εHf(t) is ~2ε.

Figure 5. Distribution of U-Pb ages of magmatic and metamorphic zircon populations in lower crustal xenoliths. Data sources are listed in Table 1 and ESM 1. Inherited zircons are not included. If no average estimate available, maximum age values are taken for magmatic zircons, assuming younger dates reflect resetting. Concordia ages are preferred for metamorphic zircons. The interval of 40 Ma exceeds individual analytical uncertainties.

Fig. 6. Possible thermal history of the lower crust of the Belomorian mobile belt (a) and the Great Falls Tectonic Zone (b). The dashed lines show a possible change in temperature over

time in the lower crust. T_c is the "closure" temperature of isotopic exchange for garnet. LC, MC and UC are the lower, middle and upper crust, respectively. **a**: Temperature estimated from Zr content in rutile is taken as the temperature of metamorphic zircon formation (Koreshkova et al., 2014, 2017). The periods of cooling after zircon formation are probable since zircon grains preserved complex textures. The cooling rate is 4°/Myr. Not all zircon data are shown. The metamorphic age distribution for the whole xenolith suite is shown in Fig. 7a. The data for the upper crust are from Balagansky et al. (2015), Bibikova et al. (2004), Daly et al. (2006), Mints et al. (2007) and Nironen (2017). **b**: Temperature estimated from Ti content in zircon is taken as the temperature of metamorphic zircon formation for samples LSC 72, LSC 89 and LSC 105 (Thakurdin et al., 2019). Thermobarometric estimates are reported for metamorphic zircons from Grt-clinopyroxenite xenolith RRE5a (Scherer et al., 2000) and monazites from middle crustal xenoliths and the lower crustal Grt-granulite xenolith ROB1 (Barnhart et al., 2012). The data for magmatic zircons are from Bolhar et al. (2007) and Thakurdin et al. (2019). U-Pb rutile data are from Blackburn et al. (2011). The data for the upper-middle crust are from Barnhart et al. (2012) and Thakurdin et al. (2019).

Figure 7. Distribution of U-Pb ages of metamorphic zircon generations in xenoliths from the Belomorian mobile belt (a) and the Daldyn and Alakit kimberlite fields in Siberia (b). Data sources are listed in Table 1 and ESM 1. The interval of 20 Ma is comparable to uncertainties of age determinations.

Table:

Table 1. Data compilation for lower crustal xenoliths from North America, Siberia and Northern Europe. Abbreviations: C – convoluted texture, H – homogeneous texture, FS – fir-tree sector-zoning, O – oscillatory texture, PS – polygonal sector-zoning, S – sector-zoning; c – core, r – rim, ov – overgrowths; m – migmatitic, n/d – not determined. Comma divides different generations.

Supplementary material:

ESM 1. Data compilation for upper-middle crustal and lower crustal xenoliths from North America, Siberia and Northern Europe.

ESM 2. General geological information about xenoliths localities.

ESM 3. εHf(t) vs U–Pb zircon age in xenoliths from kimberlites of the Markha terrane, Siberian craton.

ESM 4. Description of xenoliths from the Nakyn and Alakit kimberlite fields of the Markha terrane, Siberian craton, U-Pb data and zircon composition.

Table 1. Data compilation for lower crustal xenoliths from North America, Siberia and Northern Europe

Locality/ *data source*	Lithology	Zircon						rutile	wr T_{DM}	wr T_{DM}
		inherited age, Ga	protolith age, Ga	texture	εHf(t)	metamorphic age, Ga	texture	εHf(t)	age, Ga	Nd, Ga	Hf, Ga
North America											
Slave craton	felsic Grt-granulites	3.2-2.7 O c	2.62	H c, ov		2.56	PS, H c-r				
Davis et al., 2003	Grt-gneisses		2.97-2.62	O c		2.64-2.58	PS, H c-r		1.94-1.81		
	mafic Grt-granulite		2.64	c		2.55	r				
	mafic Grt-granulite		3.02	O c		2.78, 2.57	H r		1.39-1.06		
	mafic Grt-granulite		>2.56	c		2.51	ov		~1.1		
	mafic Grt-granulite					2.60-2.59	H				
	mafic Grt-granulite		≥2.67	H		2.56-2.53	S-H r				
Förster et al., 2017									1.3-1.1		
Wyoming craton and GFTZ											
Bolhar et al., 2007	charnockite/granulite		3.00-2.50	H c		2.17-1.76	H r				
Scherer et al., 2000	Grt-clinopyroxenite					1.71	H	-10			
Thakurdin et al., 2019a,b	mafic Grt-granulites		~3.2	H c	-4	1.77	H r				
	Grt-free granulites		≥2.53	patchy c	-3	1.84, 1.79, 1.73	H	4, -8, -19			
Farmer et al., 2005	mafic granulites		2.70-2.56	O c		1.07	H r				
Mirnejad and Bell, 2008	mafic granulites									3.78-2.66	
Medicine Hat Block											
Blackburn et al., 2011	mafic Grt-granulite								~1.0		
Superior craton											
Zartman et al., 2012	Grt-granulite	3.51, ≥2.31		O, patchy c		1.39, 1.10	O m, H r			3.26	3.75
	mafic Grt-granulites									2.11-2.26	4.88-2.95
Moser and Heaman, 1997	Pl-rich Grt-granulite					2.58, 2.50, 1.44	H				
	Pl-rich Grt-granulite		≥2.69	c		2.56, 2.50	PS c, H r				
	Pl-rich Grt-granulite		2.79	O S c		2.42	H r				
	Grt- clinopyroxenite		≥2.63	c		≤2.53	ov				
Yavapai and Mazatzal provinces	(the Colorado Plateau)										
Crowley et al., 2006	mafic Grt-granulite		≥1.43	patchy c	4-7	1.41	Feathery	7-11		1.80	1.73
	mafic Grt-granulite		≥1.43	S, patchy c	8	1.41-1.38	FS, H r	-0.5-2.5			
	mafic Grt-granulites					1.41-1.39	FS, H r	6-7			
	felsic Grt-granulites		1.73-1.60	O c	8-12	1.41-1.38	S, H, H r	0.6-14		1.76	1.60
Cheyenne belt											
Farmer et al., 2005	mafic Grt-granulites	3.2-2.6	≥1.72	O, patchy c		1.7-1.6, 1.38-1.34	FS c, H r				
Northern Europe											
Karelian craton											
Peltonen et al., 2006,	mafic Grt-granulite		3.48	O c		1.86-1.78	H			3.00	
Hölltä et al., 2000	mafic Grt-granulite	3.53 O	2.71	S c		~1.84-?	H			3.37	
	mafic Grt-granulite		2.50-1.81	O, S c		1.72	H			2.29	
	mafic Grt-granulite					1.85-1.72	H				

Table 1. Continued

Locality/ *data source*	Lithology	Zircon							rutile	wr	wr
		inherited age, Ga	protolith age, Ga	texture	εHf(t)	metamorphic age, Ga	texture	εHf(t)	age, Ga	T_{DM} Nd, Ga	T_{DM} Hf, Ga
	mafic Grt-granulite					1.98-1.77	C, H r			2.31	
	mafic Grt-granulite		≥2.67	O-H c		~1.78	H r			2.68	
Belomorian mobile belt											
Downes et al., 2002	Grt-granulite	2.84 O c	2.47	c						2.60	3.26
	mafic Grt-granulite					1.77-1.61	H			2.61	2.75
Vetrin et al., 2009	Grt-granulite		≥2.72	Patchy c	1	~1.73	H r	-8		2.72	
	Grt-granulite	2.79? S c	2.79, 2.74	O c	-3 to 3	~1.58	H r	-25		2.57	
	Grt-granulite					1.76, 1.68-1.44	H c, H r	-16 to -10		2.68	
Koreshkova et al., 2017	mafic Grt-granulite					≥2.25, 1.92, 1.86, 1.76	PS c, FS, H, C ov	-4, -10 to-15		2.66	
	mafic Grt-granulite					1.91–1.71	PS c, H r			3.26	
	mafic Grt-granulite					1.66	H			3.16	
	mafic Grt-granulite					1.77, 1.64	FS c, H r	-5, -9			
	mafic Grt-granulite					1.74, 1.6-1.3	S c, H r	-7		2.26	
	Grt-websterite					1.70-1.65	S c, H r	-7			
	Prg-Phl-eclogite					1.65-1.27	H	-13 to-21			
	Grt-Phl-rock					1.66	H	-16			
	Grt-Opx-Phl-rock					1.76, 1.71-1.60	S c, H r				
	Phl-clinopyroxenite		1.64	S							
	mafic Grt-granulites									3.14-2.38	3.40-2.80
Koreshkova et al.,2014,2017	mafic Grt-granulite	2.75 S c	2.72	O c	-1 to -5	1.81	H r	-25			
	mafic Grt-granulite					1.96, 1.82	S c, C ov	-10, -13			
	mafic Grt-granulite					1.84	S c, C ov	-8, -24			
	mafic Grt-granulite					~1.91, 1.75-1.41	Patchy c, H r				
	Grt-Phl-clinopyroxenite					1.93, 1.77	FS c, H r				
Siberia											
Anabar province of the Siberian craton											
The Alakit field											
Shatsky et al., 2016	mafic Grt-granulite					1.86	H	-9 to -6			
this study	mafic Grt-granulite					≥2.04, 1.66	S				
The Daldyn field											
Koreshkova et al., 2009	mafic Grt-granulite		3.15	O c		1.83	H r			3.31	4.02
	mafic Grt-granulite		2.71	O c		1.82	H r			2.85	2.98
	mafic Grt-granulite					1.83	C				
	mafic Grt-granulite					1.81	H r			2.55	
	mafic Grt-granulite					1.94, 1.87	FS, C ov			3.09	3.71
	mafic Grt-granulite					1.85	C ov			2.72	3.24
	mafic Grt-granulite		>2.05	O c		1.90, ~1.84	H, c			1.34	

Table 1. Continued

Locality/ *data source*	Lithology	Zircon							rutile	wr T_{DM}	wr T_{DM}
		inherited age, Ga	protolith age, Ga	texture	εHf(t)	metamorphic age, Ga	texture	εHf(t)	age, Ga	Nd, Ga	Hf, Ga
Shatsky et al., 2016	mafic Grt-granulite		≥2.53	Patchy c	-5 to -4	1.78	H	-23			
	mafic Grt-granulite					1.79	H?	1-2			
	mafic Grt-granulite		>1.99	c	-12	~1.98, ~1.88	H?, H r	-4 to -1			
Moyen et al., 2017	mafic Grt-granulite		2.66	c		1.85	r				
	mafic Grt-granulite		2.9-2.7	c		1.85	r				
	mafic Grt-granulite		2.71	c		n/d	r				
	mafic Grt-granulite					1.83	c, r	-9			
	mafic Grt-granulite					1.84	S c, r	-3			
	mafic Grt-granulite					1.84	c, r	-19			
Shatsky et al., 2019	Grt-free granulite	2.87 S c	2.86, 2.67	O c	1, 0	2.42?, n/d	H, H r	-6, n/d		2.77	
	Grt-free granulite		2.68-2.64	O c	-3 - 0	~1.90	H r	-16		3.02	
	mafic Grt-granulite		≥2.58	O c	-4	n/d, 1.82-1.80	H, C ov	-19		3.16	
Muna field											
Shatsky et al., 2018	mafic Grt-granulite	≥2.74 O c	2.73	O c	1	n/d	H r				
	Grt-granulite	≥2.72 O c	2.72	O c	-2	n/d	r				
	Grt-free granulite	≥2.72 O c	2.71	O c	0	n/d	r				
Rosen et al., 2006	mafic Grt-granulite		3.19	c		1.86				2.93	
Nakyn field											
Shatsky et al., 2018	Grt-granulite	2.94 H c	2.89-2.87	O c	0-6	n/d	H r				
	Grt-granulite		2.77-2.75	c	0-3	≤2.04	H r	-16			
this study	mafic Grt-granulite					1.85	C				
	mafic Grt-granulite					1.88	FS-C				

Abbreviations: C – convoluted texture, H – homogeneous texture, FS – fir-tree sector-zoning, O – oscillatory texture, PS – polygonal sector-zoning, S – sector-zoning; c – core, r – rim, ov – overgrowths; m – migmatitic, n/d – not determined. Comma divides different generations.

Declaration of interests

☒ The authors declare that they have no known competing financial interests or personal relationships that could have appeared to influence the work reported in this paper.

☐The authors declare the following financial interests/personal relationships which may be considered as potential competing interests:

CRediT author statement

Marina Koreshkova and Hilary Downes made equal contributions to the manuscript.

Figure

Click here to access/download;Figure;Fig1.tif

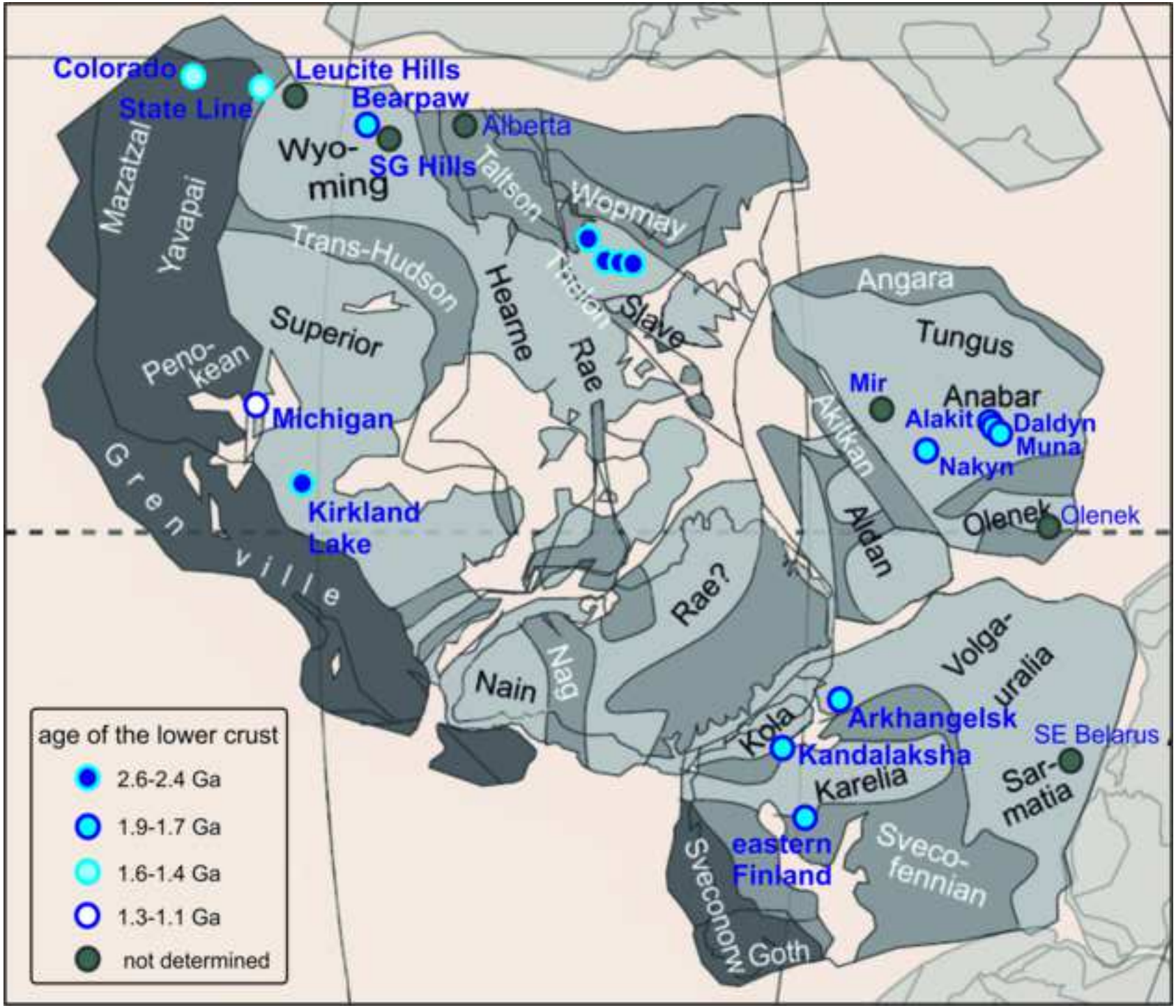

Figure

Click here to access/download;Figure;Fig2.tif

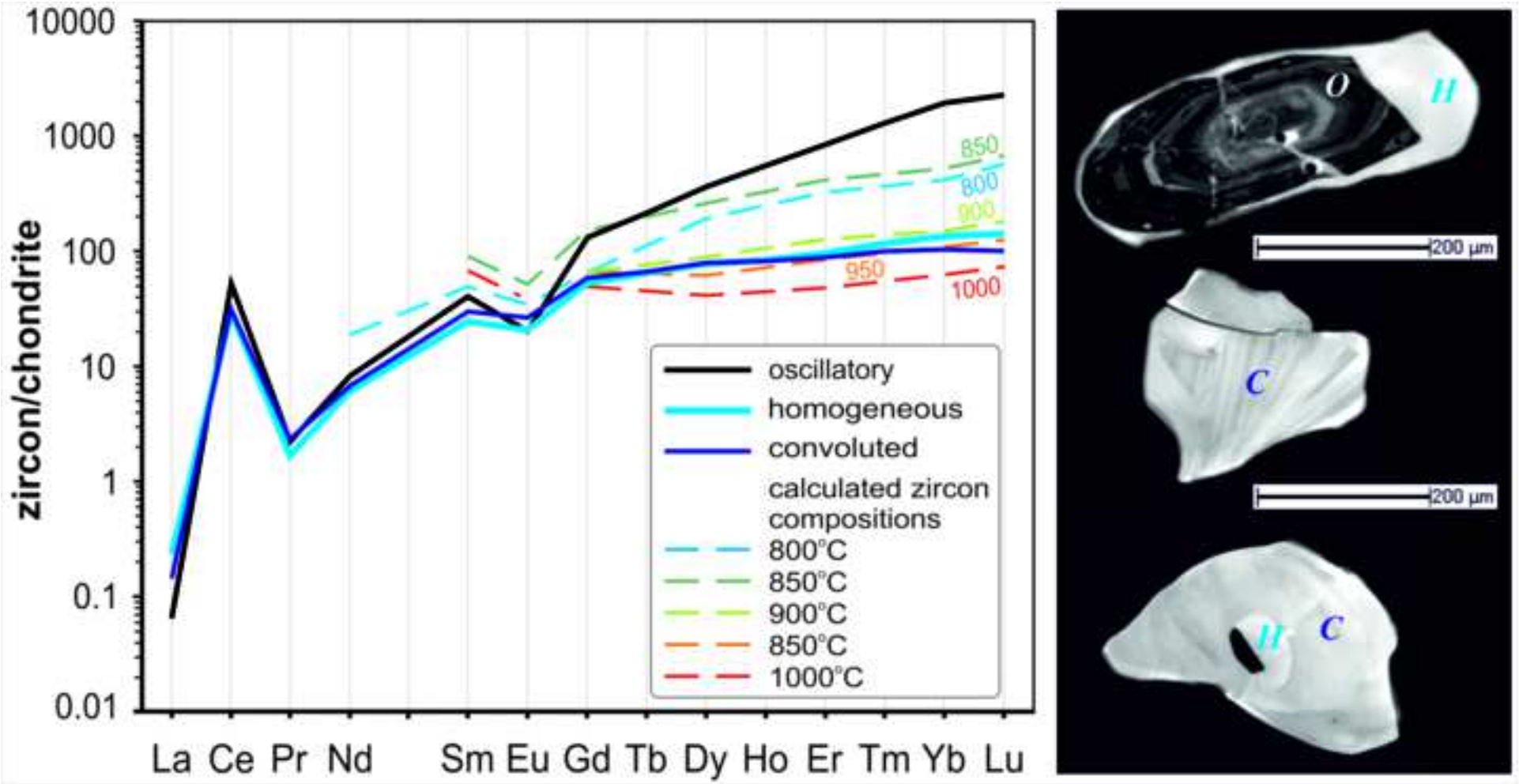

Figure

Click here to access/download;Figure;Fig3 new.tif

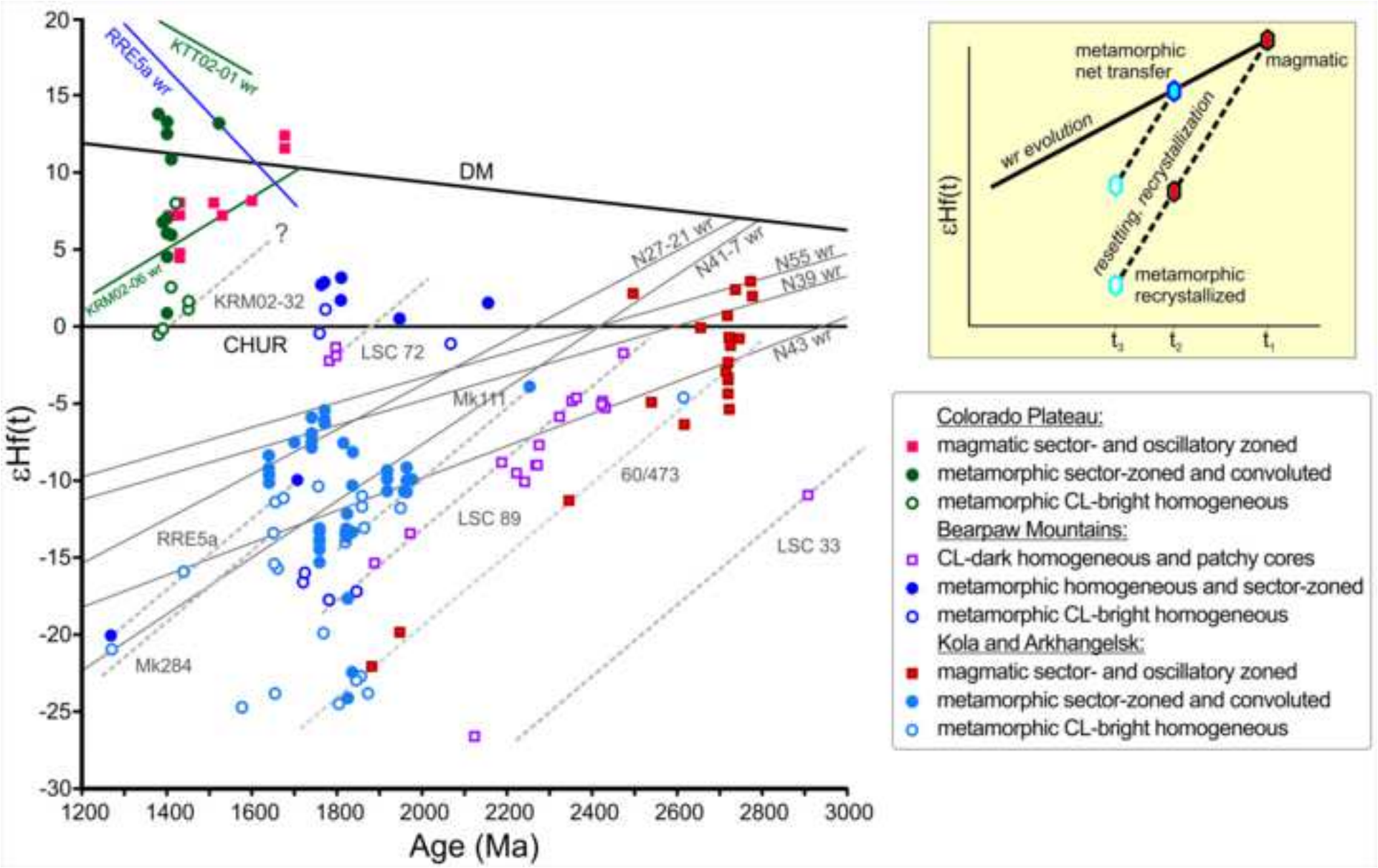

Figure

Click here to access/download;Figure;Fig4.tif

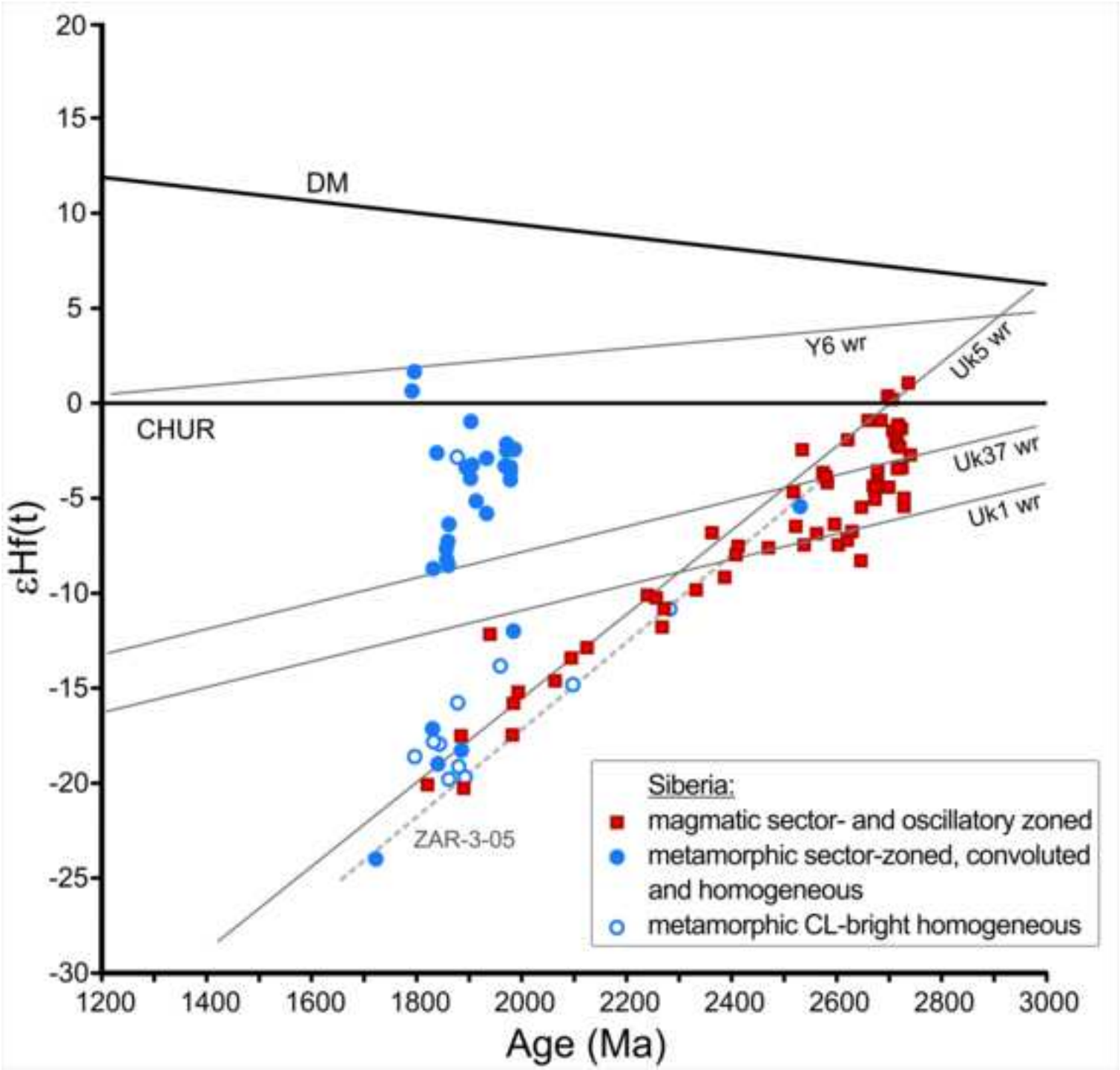

Figure

Click here to access/download;Figure;Fig5.tif

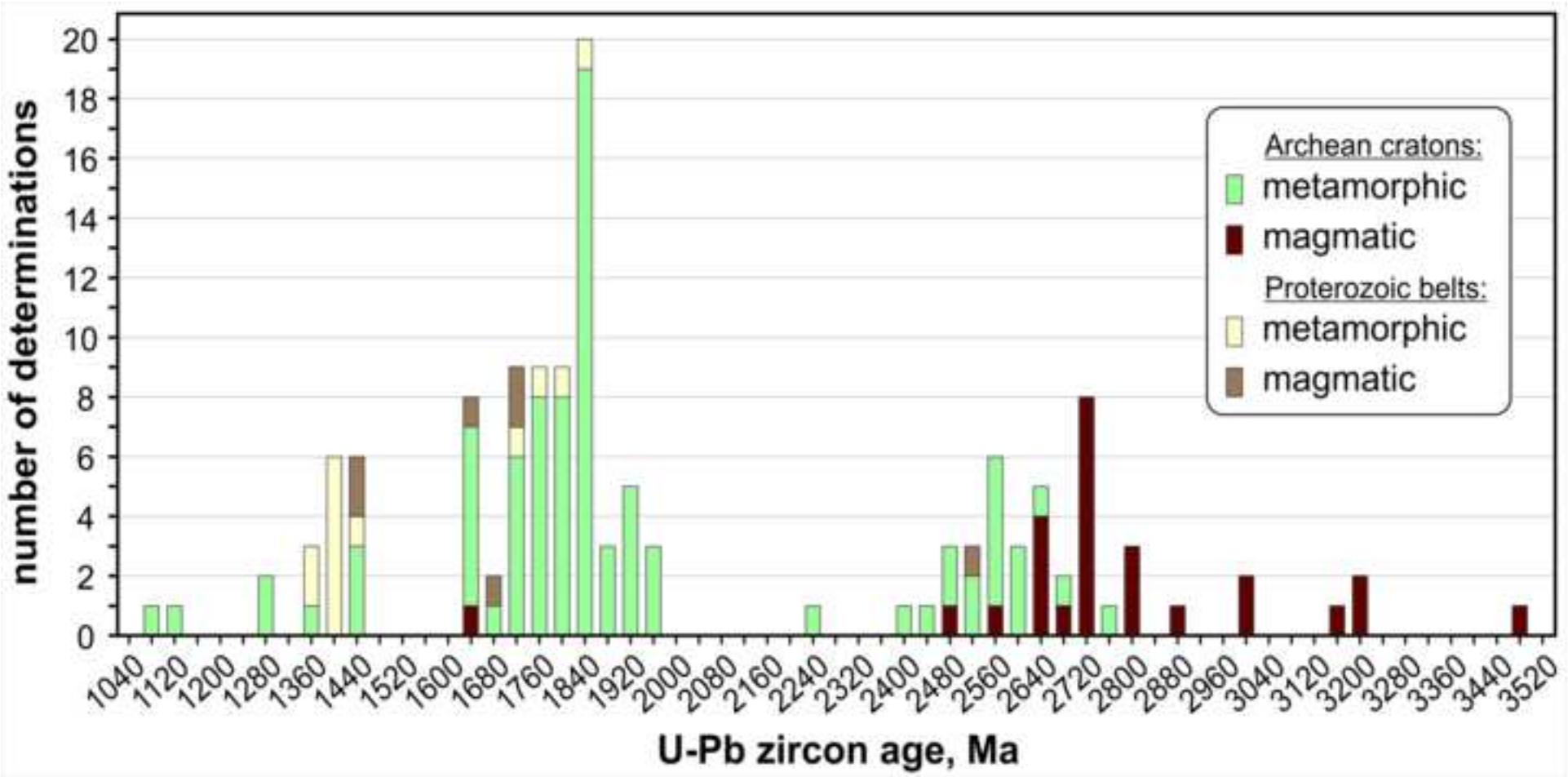

Figure

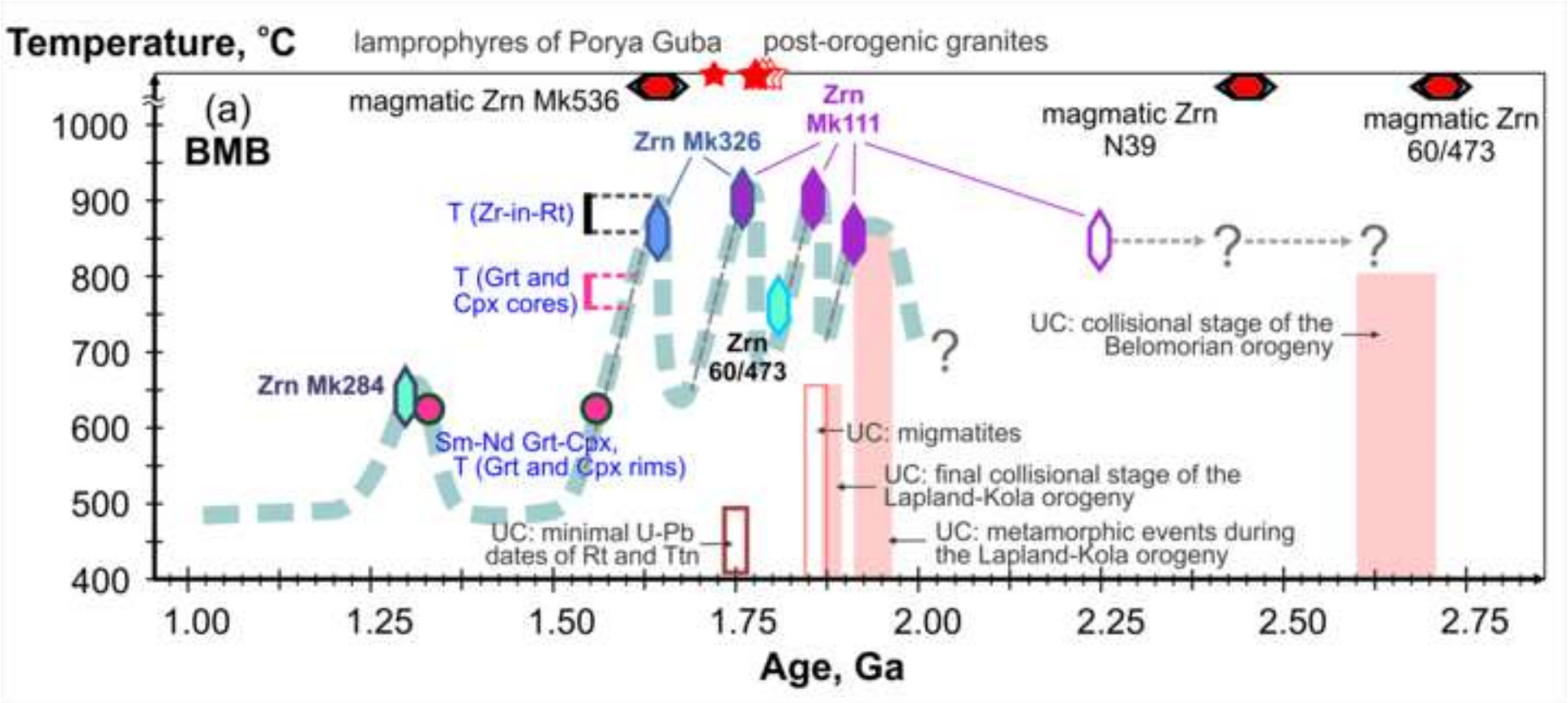

Figure

Click here to access/download;Figure;Fig6b.tif

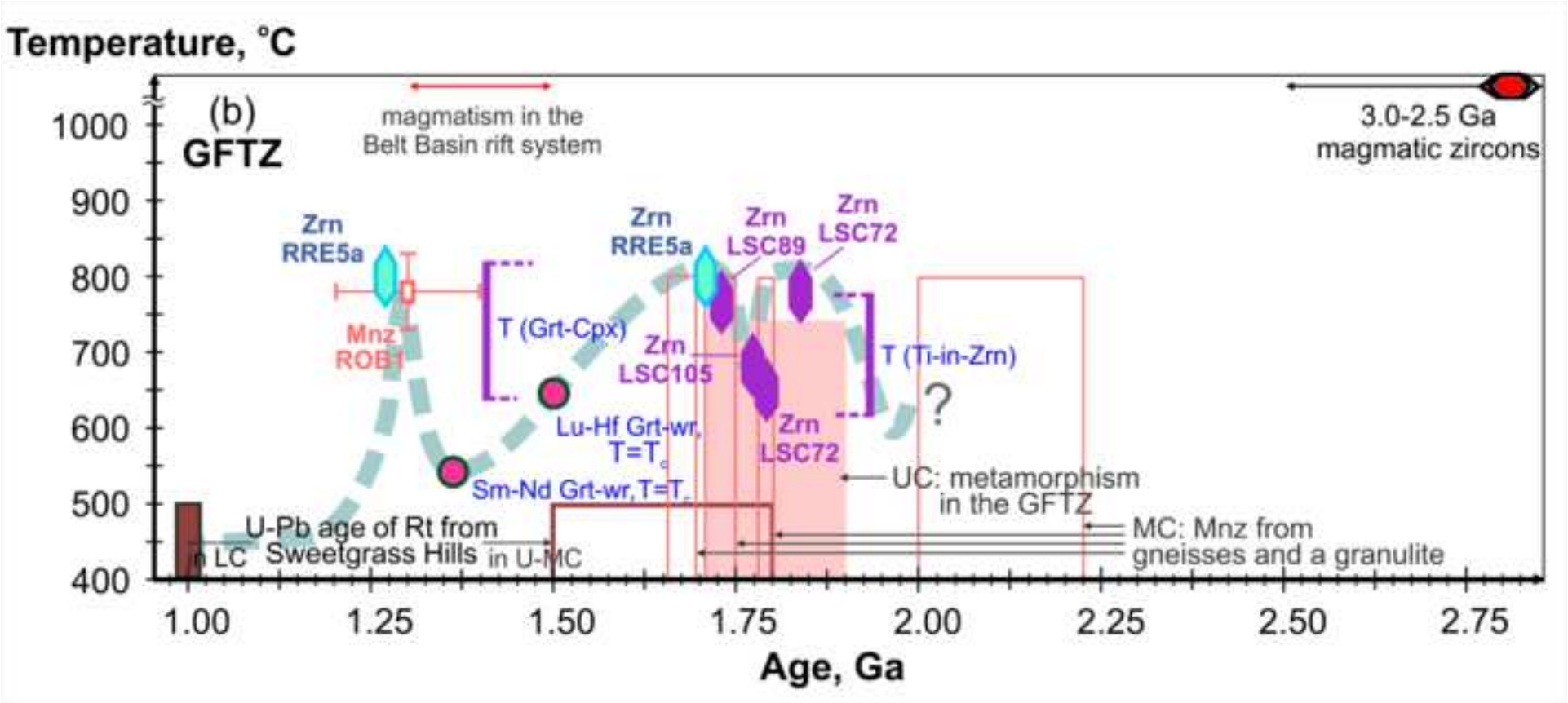

Figure

Click here to access/download;Figure;Fig7.tif

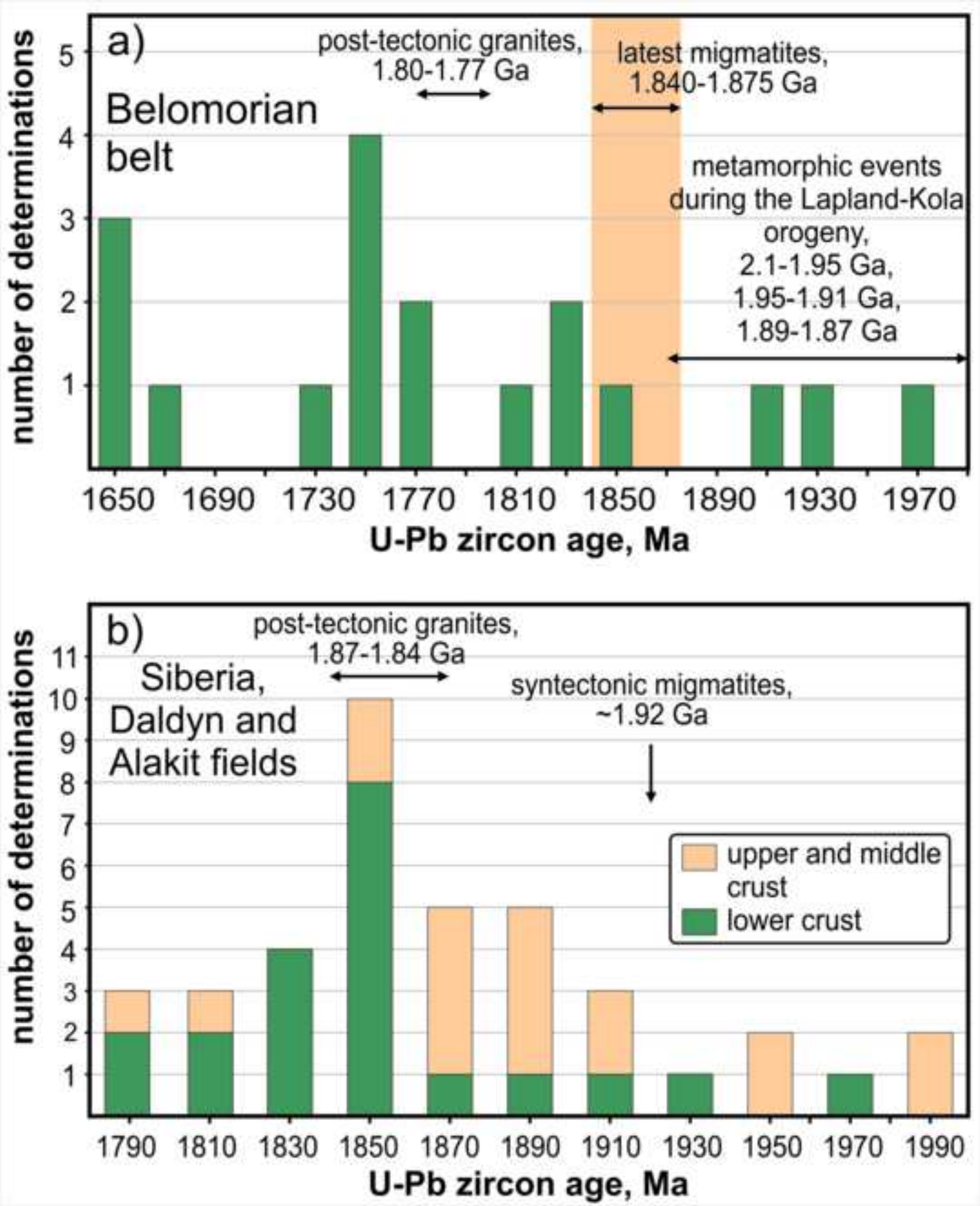

Table 1. Data compilation for lower crustal xenoliths from North America, Siberia and Northern Europe

Locality/ *data source*	Lithology	Zircon						rutile	wr T_{DM}	wr T_{DM}
		inhereted age, Ga	protolith age, Ga	texture	εHf(t)	metamorphic age, Ga	texture	εHf(t)	age, Ga	Nd, Ga	Hf, Ga
North America											
Slave craton	felsic Grt-granulites	3.2-2.7 O c	2.62	H c, ov		2.56	PS, H c-r				
Davis et al., 2003	Grt-gneisses		2.97-2.62	O c		2.64-2.58	PS, H c-r		1.94-1.81		
	mafic Grt-granulite		2.64	c		2.55	r				
	mafic Grt-granulite		3.02	O c		2.78, 2.57	H r		1.39-1.06		
	mafic Grt-granulite		>2.56	c		2.51	ov		~1.1		
	mafic Grt-granulite					2.60-2.59	H				
	mafic Grt-granulite		≥2.67	H		2.56-2.53	S-H r				
Förster et al., 2017									1.3-1.1		
Wyoming craton and GFTZ											
Bolhar et al., 2007	charnockite/granulite		3.00-2.50	H c		2.17-1.76	H r				
Scherer et al., 2000	Grt-clinopyroxenite					1.71	H	-10			
Thakurdin et al., 2019a,b	mafic Grt-granulites		~3.2	H c	-4	1.77	H r				
	Grt-free granulites		≥2.53	patchy c	-3	1.84, 1.79, 1.73	H	4, -8, -19			
Farmer et al., 2005	mafic granulites		2.70-2.56	O c		1.07	H r				
Mirnejad and Bell, 2008	mafic granulites									3.78-2.66	
Medicine Hat Block											
Blackburn et al., 2011	mafic Grt-granulite								~1.0		
Superior craton											
Zartman et al., 2012	Grt-granulite	3.51, ≥2.31		O, patchy c		1.39, 1.10	O m, H r			3.26	3.75
	mafic Grt-granulites									2.11-2.26	4.88-2.95
Moser and Heaman, 1997	Pl-rich Grt-granulite					2.58, 2.50, 1.44	H				
	Pl-rich Grt-granulite		≥2.69	c		2.56, 2.50	PS c, H r				
	Pl-rich Grt-granulite		2.79	O S c		2.42	H r				
	Grt- clinopyroxenite		≥2.63	c		≤2.53	ov				
Yavapai and Mazatzal provinces	(the Colorado Plateau)										
Crowley et al., 2006	mafic Grt-granulite		≥1.43	patchy c	4-7	1.41	Feathery	7-11		1.80	1.73
	mafic Grt-granulite		≥1.43	S, patchy c	8	1.41-1.38	FS, H r	-0.5-2.5			
	mafic Grt-granulites					1.41-1.39	FS, H r	6-7			
	felsic Grt-granulites		1.73-1.60	O c	8-12	1.41-1.38	S, H, H r	0.6-14		1.76	1.60
Cheyenne belt											
Farmer et al., 2005	mafic Grt-granulites	3.2-2.6	≥1.72	O, patchy c		1.7-1.6, 1.38-1.34	FS c, H r				
Northern Europe											
Karelian craton											
Peltonen et al., 2006,	mafic Grt-granulite		3.48	O c		1.86-1.78	H			3.00	
Hölltä et al., 2000	mafic Grt-granulite	3.53 O	2.71	S c		~1.84-?	H			3.37	
	mafic Grt-granulite		2.50-1.81	O, S c		1.72	H			2.29	
	mafic Grt-granulite					1.85-1.72	H				

Table 1. Continued

Locality/ *data source*	Lithology	Zircon							rutile	wr	wr
		inhereted age, Ga	protolith age, Ga	texture	εHf(t)	metamorphic age, Ga	texture	εHf(t)	age, Ga	T_{DM} Nd, Ga	T_{DM} Hf, Ga
	mafic Grt-granulite					1.98-1.77	C, H r			2.31	
	mafic Grt-granulite		≥2.67	O-H c		~1.78	H r			2.68	
Belomorian mobile belt											
Downes et al., 2002	Grt-granulite	2.84 O c	2.47	c						2.60	3.26
	mafic Grt-granulite					1.77-1.61	H			2.61	2.75
Vetrin et al., 2009	Grt-granulite		≥2.72	Patchy c	1	~1.73	H r	-8		2.72	
	Grt-granulite	2.79? S c	2.79, 2.74	O c	-3 to 3	~1.58	H r	-25		2.57	
	Grt-granulite					1.76, 1.68-1.44	H c, H r	-16 to -10		2.68	
Koreshkova et al., 2017	mafic Grt-granulite					≥2.25, 1.92, 1.86, 1.76	PS c, FS, H, C ov	-4, -10 to-15		2.66	
	mafic Grt-granulite					1.91–1.71	PS c, H r			3.26	
	mafic Grt-granulite					1.66	H			3.16	
	mafic Grt-granulite					1.77, 1.64	FS c, H r	-5, -9			
	mafic Grt-granulite					1.74, 1.6-1.3	S c, H r	-7		2.26	
	Grt-websterite					1.70-1.65	S c, H r	-7			
	Prg-Phl-eclogite					1.65-1.27	H	-13 to-21			
	Grt-Phl-rock					1.66	H	-16			
	Grt-Opx-Phl-rock					1.76, 1.71-1.60	S c, H r				
	Phl-clinopyroxenite		1.64	S							
	mafic Grt-granulites									3.14-2.38	3.40-2.80
Koreshkova et al.,2014,2017	mafic Grt-granulite	2.75 S c	2.72	O c	-1 to -5	1.81	H r	-25			
	mafic Grt-granulite					1.96, 1.82	S c, C ov	-10, -13			
	mafic Grt-granulite					1.84	S c, C ov	-8, -24			
	mafic Grt-granulite					~1.91, 1.75-1.41	Patchy c, H r				
	Grt-Phl-clinopyroxenite					1.93, 1.77	FS c, H r				
Siberia											
Anabar province of the Siberian craton											
The Alakit field											
Shatsky et al., 2016	mafic Grt-granulite					1.86	H	-9 to -6			
this study	mafic Grt-granulite					≥2.04, 1.66	S				
The Daldyn field											
Koreshkova et al., 2009	mafic Grt-granulite		3.15	O c		1.83	H r			3.31	4.02
	mafic Grt-granulite		2.71	O c		1.82	H r			2.85	2.98
	mafic Grt-granulite					1.83	C				
	mafic Grt-granulite					1.81	H r			2.55	
	mafic Grt-granulite					1.94, 1.87	FS, C ov			3.09	3.71
	mafic Grt-granulite					1.85	C ov			2.72	3.24
	mafic Grt-granulite		>2.05	O c		1.90, ~1.84	H, c			1.34	

Table 1. Continued

Locality/ *data source*	Lithology	Zircon							rutile	wr T_{DM}	wr T_{DM}
		inhereted age, Ga	protolith age, Ga	texture	εHf(t)	metamorphic age, Ga	texture	εHf(t)	age, Ga	Nd, Ga	Hf, Ga
Shatsky et al., 2016	mafic Grt-granulite		≥2.53	Patchy c	-5 to -4	1.78	H	-23			
	mafic Grt-granulite					1.79	H?	1-2			
	mafic Grt-granulite		>1.99	c	-12	~1.98, ~1.88	H?, H r	-4 to -1			
Moyen et al., 2017	mafic Grt-granulite		2.66	c		1.85	r				
	mafic Grt-granulite		2.9-2.7	c		1.85	r				
	mafic Grt-granulite		2.71	c		n/d	r				
	mafic Grt-granulite					1.83	c, r	-9			
	mafic Grt-granulite					1.84	S c, r	-3			
	mafic Grt-granulite					1.84	c, r	-19			
Shatsky et al., 2019	Grt-free granulite	2.87 S c	2.86, 2.67	O c	1, 0	2.42?, n/d	H, H r	-6, n/d		2.77	
	Grt-free granulite		2.68-2.64	O c	-3 - 0	~1.90	H r	-16		3.02	
	mafic Grt-granulite		≥2.58	O c	-4	n/d, 1.82-1.80	H, C ov	-19		3.16	
Muna field											
Shatsky et al., 2018	mafic Grt-granulite	≥2.74 O c	2.73	O c	1	n/d	H r				
	Grt-granulite	≥2.72 O c	2.72	O c	-2	n/d	r				
	Grt-free granulite	≥2.72 O c	2.71	O c	0	n/d	r				
Rosen et al., 2006	mafic Grt-granulite		3.19	c		1.86				2.93	
Nakyn field											
Shatsky et al., 2018	Grt-granulite	2.94 H c	2.89-2.87	O c	0-6	n/d	H r				
	Grt-granulite		2.77-2.75	c	0-3	≤2.04	H r	-16			
this study	mafic Grt-granulite					1.85	C				
	mafic Grt-granulite					1.88	FS-C				

Abbreviations: C – convoluted texture, H – homogeneous texture, FS – fir-tree sector-zoning, O – oscillatory texture, PS – polygonal sector-zoning, S – sector-zoning; c – core, r – rim, ov – overgrowths; m – migmatitic, n/d – not determined. Comma divides different generations.